

# ***WEAK LENSING***

## ***THE NEXT GENERATION***

ERIC HUFF (JPL)

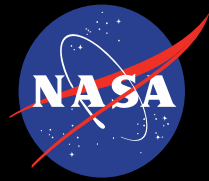
TIM EIFLER (JPL)

ERIN SHELDON (BNL)

RACHEL MANDELBAUM (CMU)



**Jet Propulsion Laboratory**  
California Institute of Technology



**Jet Propulsion Laboratory**  
California Institute of Technology

## What I'm going to talk about:

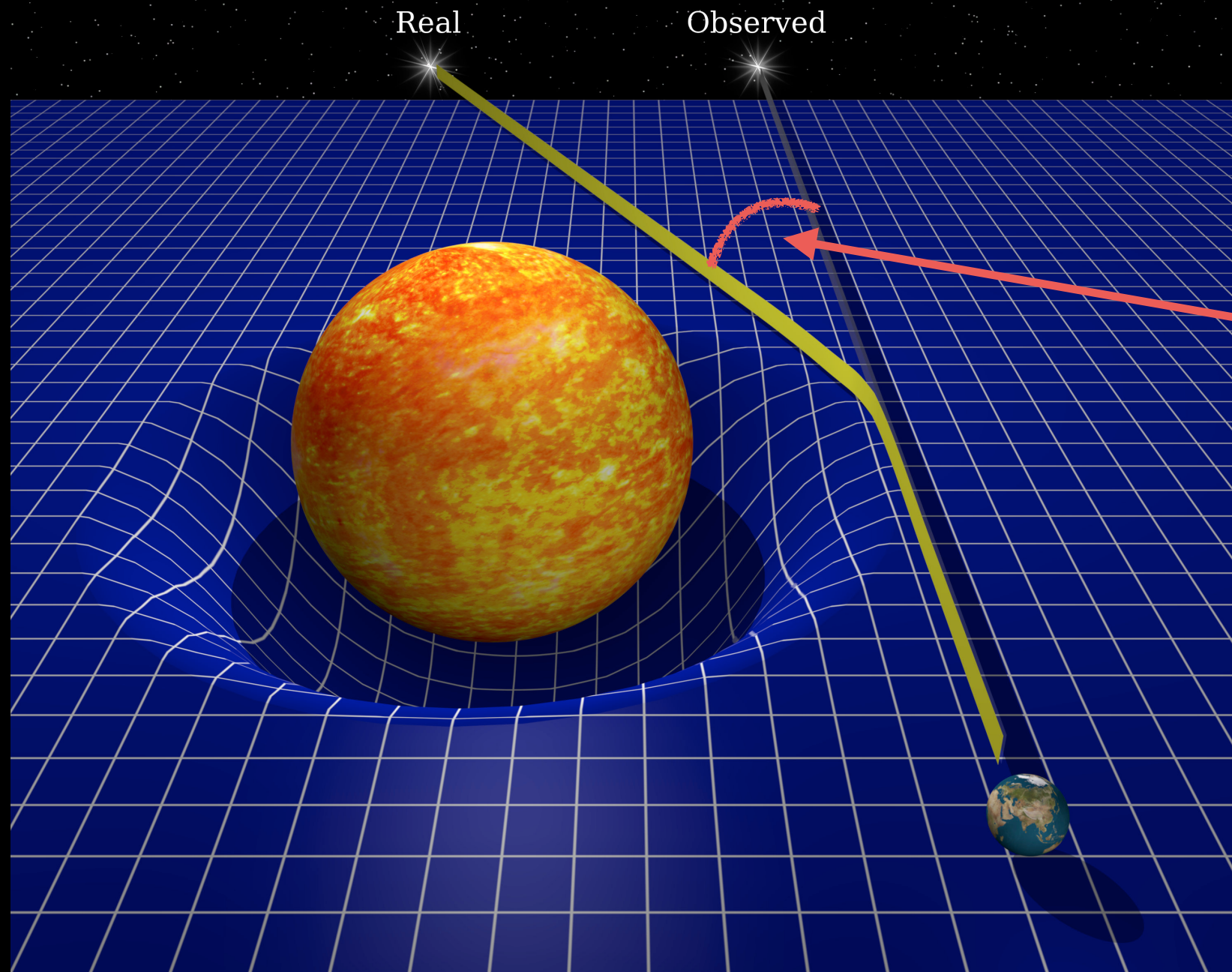
### 1. Lensing measurement:

- why it's hard
- how to solve it

### 2. Lensing from galaxy kinematics

- how it works
- how I'm hoping to measure it

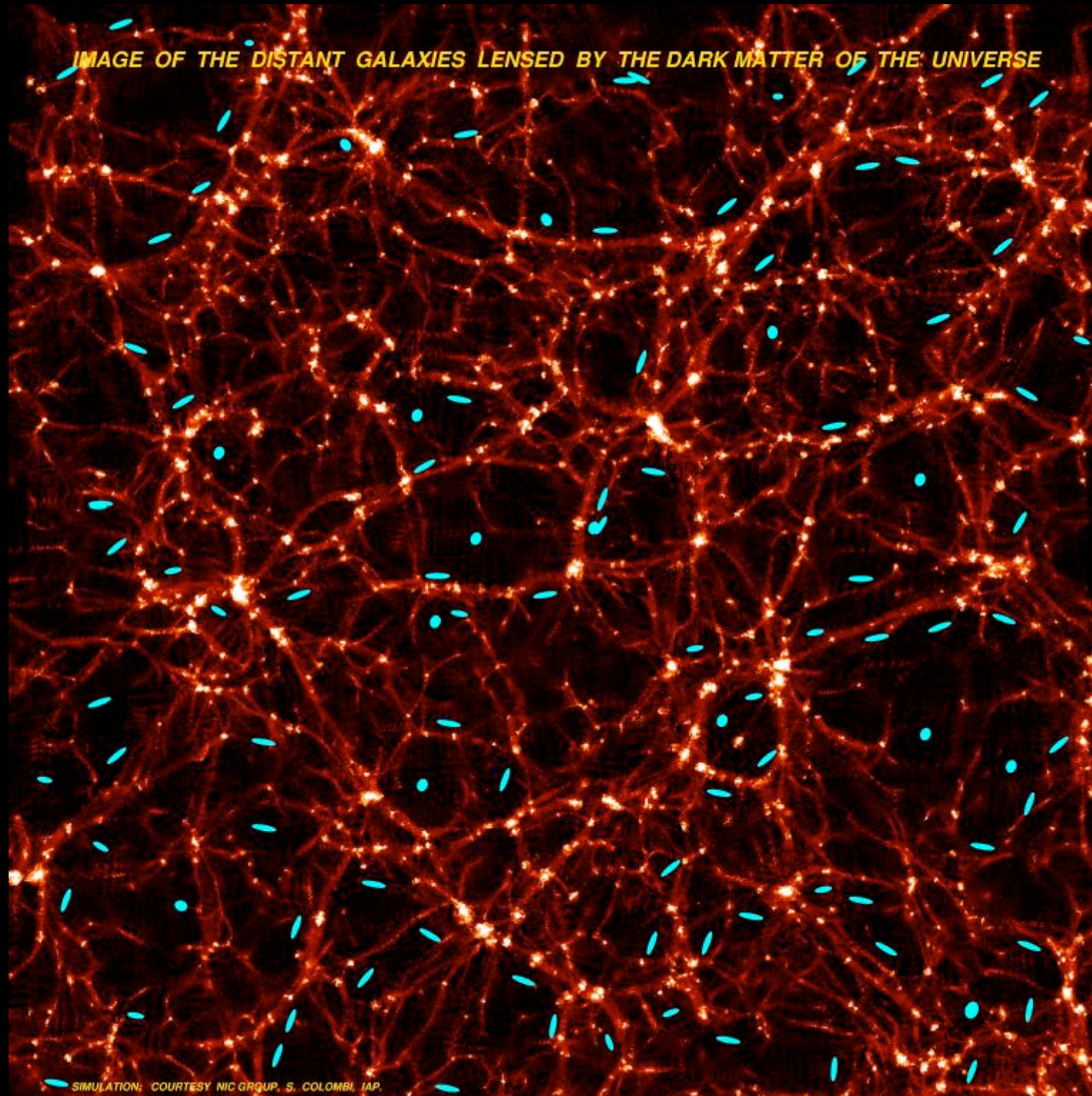
# Lensing is sensitive to both growth and geometry:



**lens mass  
and distances  
modify deflection  
angle**



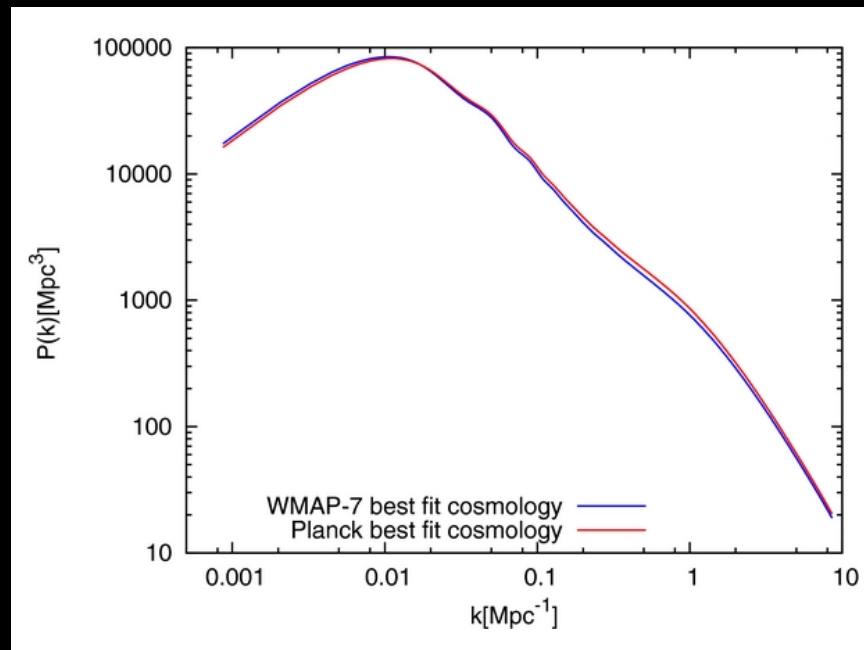
# Weak lensing is a key probe of the growth of structure.





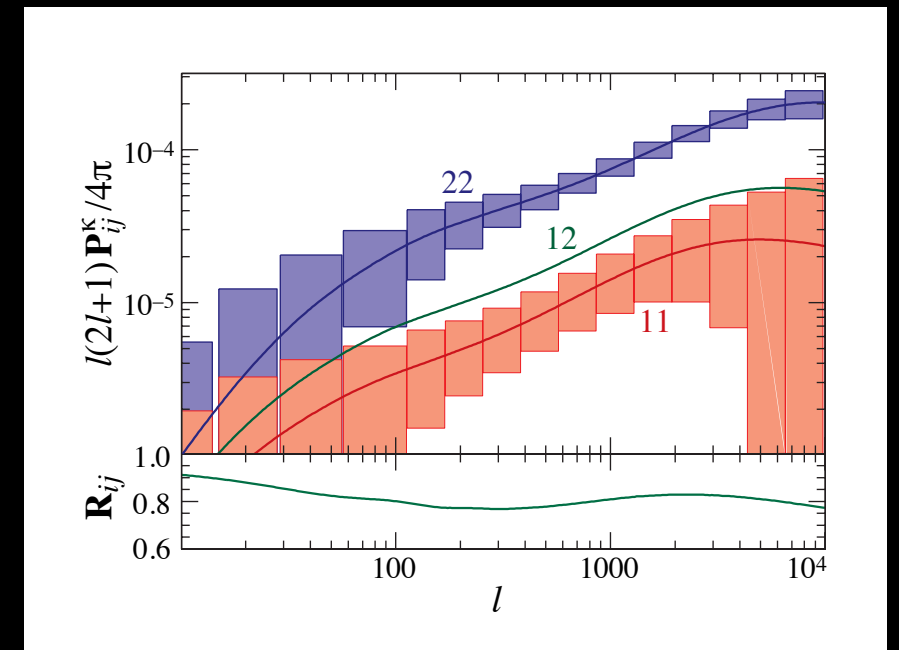
# Galaxy shape and matter fluctuations are correlated by lensing.

## Matter Power Spectrum



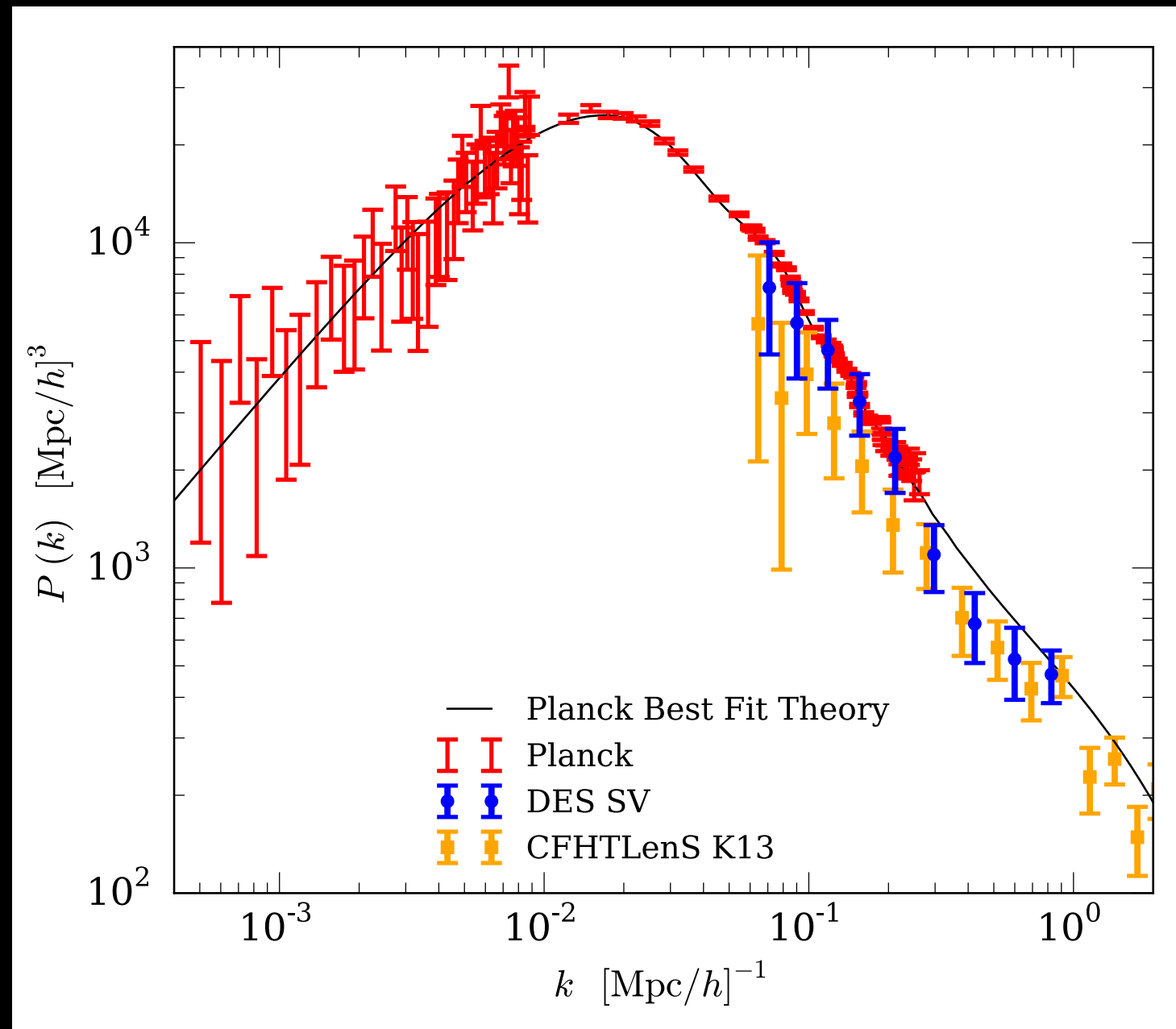
- Well understood dependence on cosmological parameters
- ‘Sharp’ features (e.g., BAO)

## Galaxy Shear Power Spectrum



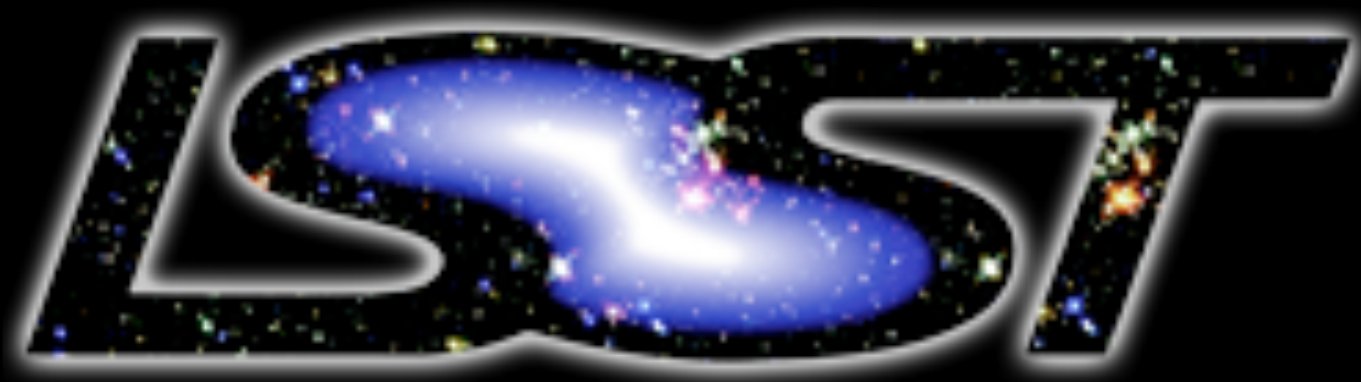
- Smooth in scale and redshift
- Weak, hard to measure
- ...but observable

# Understanding the physics of cosmic acceleration requires measuring the growth of structure.



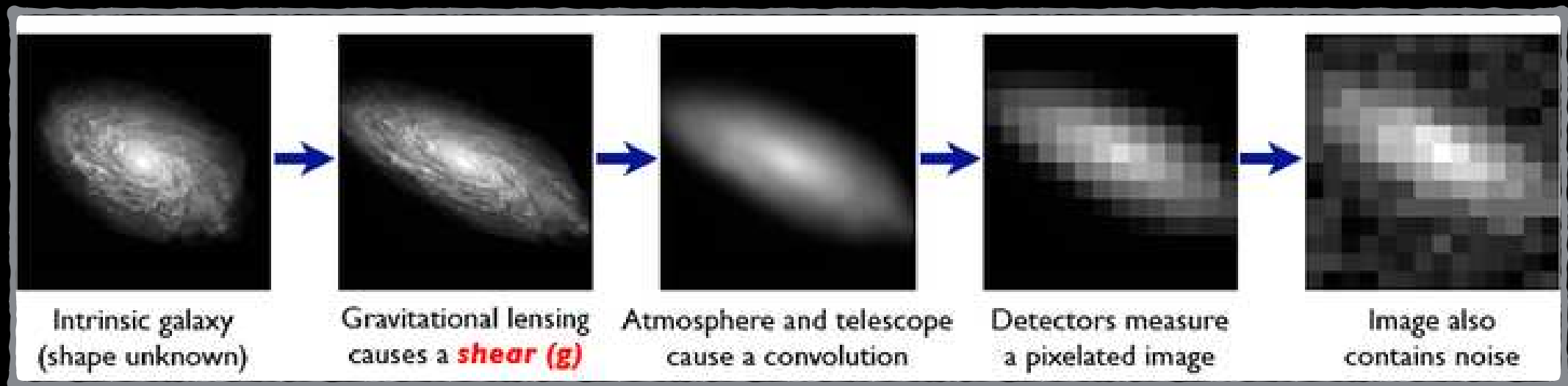
**Key signature: disagreement between early-time forecasts and late-time structure measurements**

**For this reason, lensing is a key driver of the Stage IV dark energy experiments.**





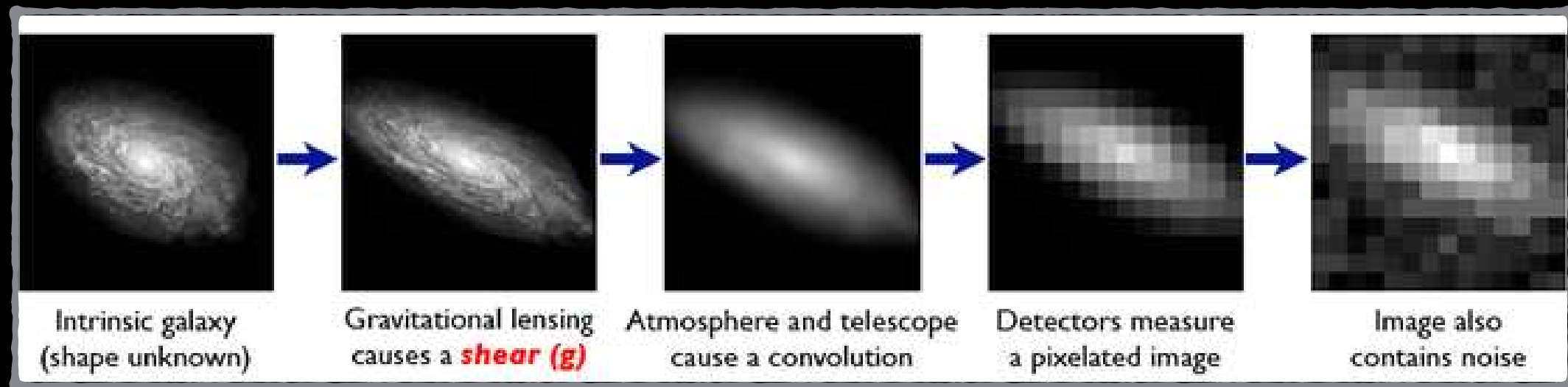
# The success of these programs depends on the accuracy of lensing shear measurement.



Bridle et al. 2008

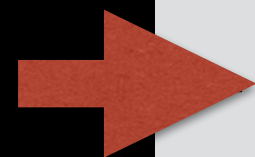
$$\Psi(\boldsymbol{\theta}) = \frac{4G}{c^2} \frac{D_l D_s}{D_{ls}} \int d^2\theta' \Sigma(\boldsymbol{\theta}') \ln |\boldsymbol{\theta} - \boldsymbol{\theta}'|,$$

# The success of these programs depends on the accuracy of lensing shear measurement.



Bridle et al. 2008

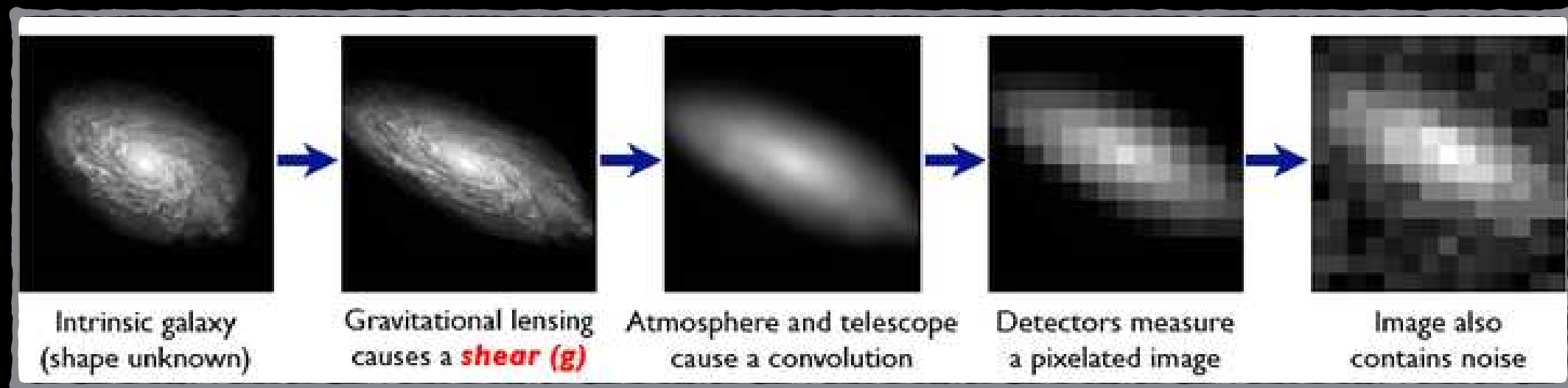
**linear(ized)  
remapping  
of the image**



$$\Psi(\boldsymbol{\theta}) = \frac{4G}{c^2} \frac{D_l D_s}{D_{ls}} \int d^2\theta' \Sigma(\boldsymbol{\theta}') \ln |\boldsymbol{\theta} - \boldsymbol{\theta}'|,$$

$$\left( \delta_{ij} - \frac{\partial^2 \Psi(\boldsymbol{\theta})}{\partial \theta_i \partial \theta_j} \right) = \begin{pmatrix} 1 - \kappa - \gamma_1 & -\gamma_2 \\ -\gamma_2 & 1 - \kappa + \gamma_1 \end{pmatrix}$$

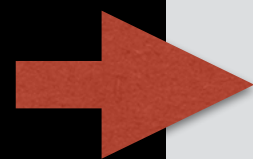
# The success of these programs depends on the accuracy of lensing shear measurement.



Bridle et al. 2008

$$\Psi(\boldsymbol{\theta}) = \frac{4G}{c^2} \frac{D_l D_s}{D_{ls}} \int d^2\theta' \Sigma(\boldsymbol{\theta}') \ln |\boldsymbol{\theta} - \boldsymbol{\theta}'|,$$
$$= \left( \delta_{ij} - \frac{\partial^2 \Psi(\boldsymbol{\theta})}{\partial \theta_i \partial \theta_j} \right) = \begin{pmatrix} 1 - \kappa - \gamma_1 & -\gamma_2 \\ -\gamma_2 & 1 - \kappa + \gamma_1 \end{pmatrix}$$

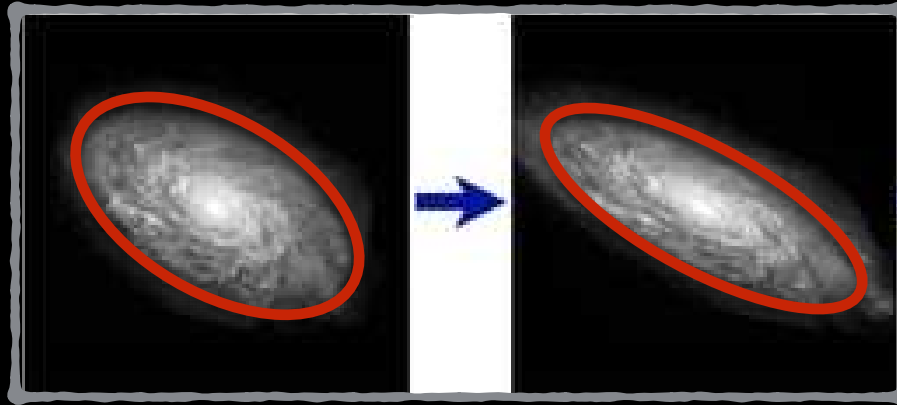
we usually  
re-parameterize  
with  $g$



$$g = \frac{\gamma}{1 - \kappa}$$



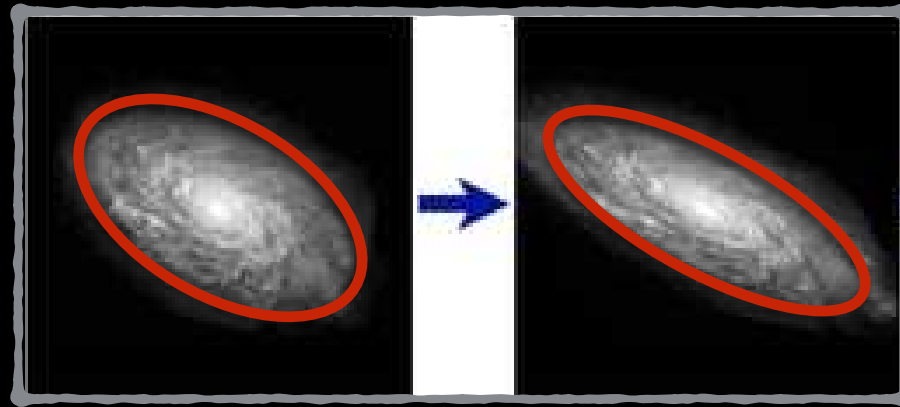
# How do we get $g$ from a galaxy image?



**ellipticity  
suggests  
2nd moments**

$$Q_{ij\dots k} = \int I(\boldsymbol{\theta})\theta_i\theta_j\dots\theta_k d^2\theta .$$
$$\chi = \frac{(Q_{11} - Q_{22}) + 2iQ_{12}}{Q_{11} + Q_{22}}$$

# How do we get $g$ from a galaxy image?

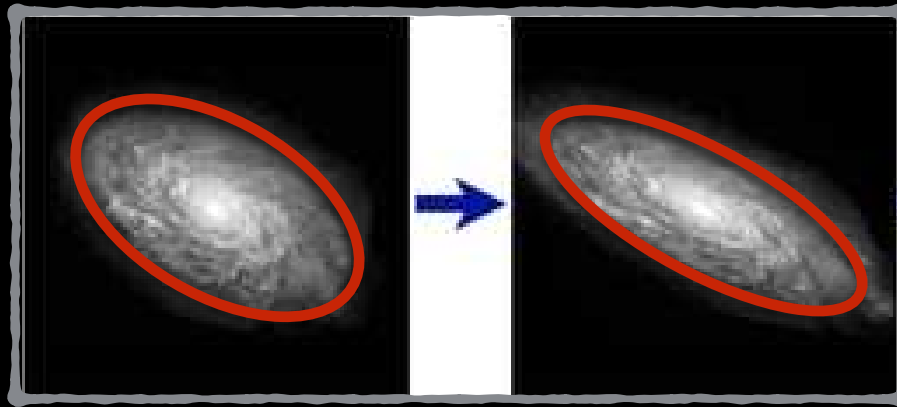


$$Q_{ij\dots k} = \int I(\boldsymbol{\theta}) \theta_i \theta_j \dots \theta_k d^2 \theta .$$
$$\chi = \frac{(Q_{11} - Q_{22}) + 2iQ_{12}}{Q_{11} + Q_{22}}$$

**$g$  and  $\chi$   
are related...**

$$g \simeq \frac{\langle \chi \rangle}{2(1 - \sigma_\chi^2)}$$

# How do we get $g$ from a galaxy image?



$$Q_{ij\dots k} = \int I(\theta)\theta_i\theta_j\dots\theta_k d^2\theta .$$
$$\chi = \frac{(Q_{11} - Q_{22}) + 2iQ_{12}}{Q_{11} + Q_{22}}$$

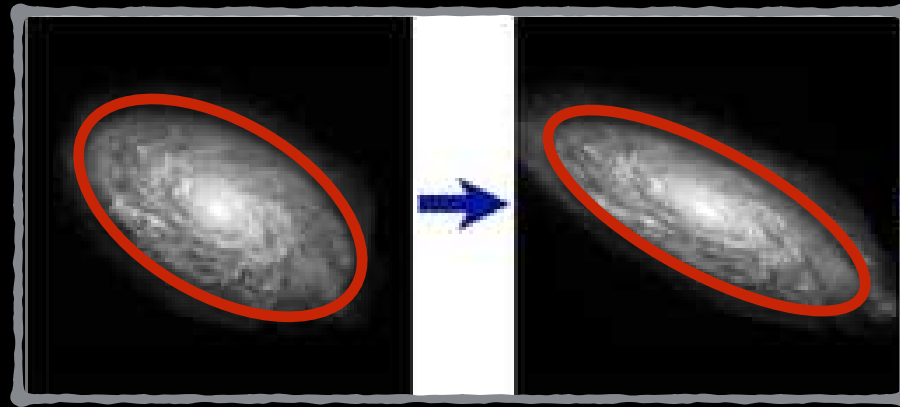
**$g$  and  $\chi$   
are related...**

$$g \simeq \frac{\langle \chi \rangle}{2(1 - \sigma_\chi^2)}$$

**...but in a way that  
depends on the ensemble.**



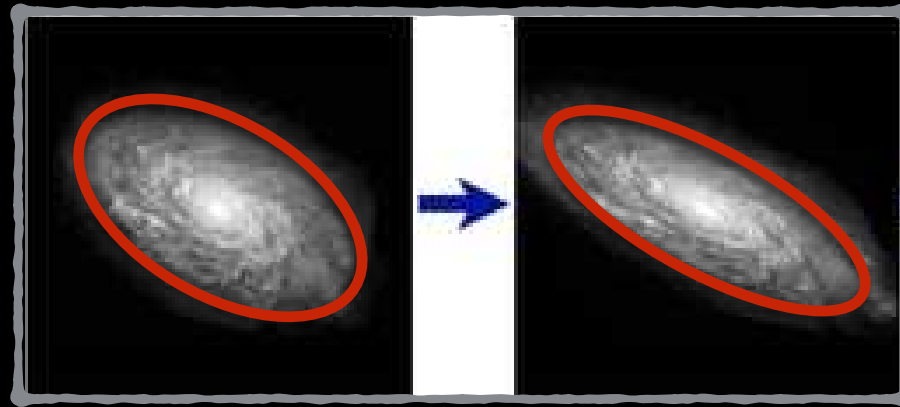
# How do we get $g$ from a galaxy image?



$$e = (1 + m)g + c$$

**preferred  
direction**

# How do we get $g$ from a galaxy image?



$$e = (1 + m)g + c$$



**calibration  
bias**

**(what all the fuss is about)**

# Kaiser, Squires, Broadhurst (1995)

1. Compute second moments.
2. Calculate the responses to shear ( $P_g$ ) and PSF ellipticity ( $P^{sm}$ ).
3. Correct for PSF ellipticity ( $e^*$ ).

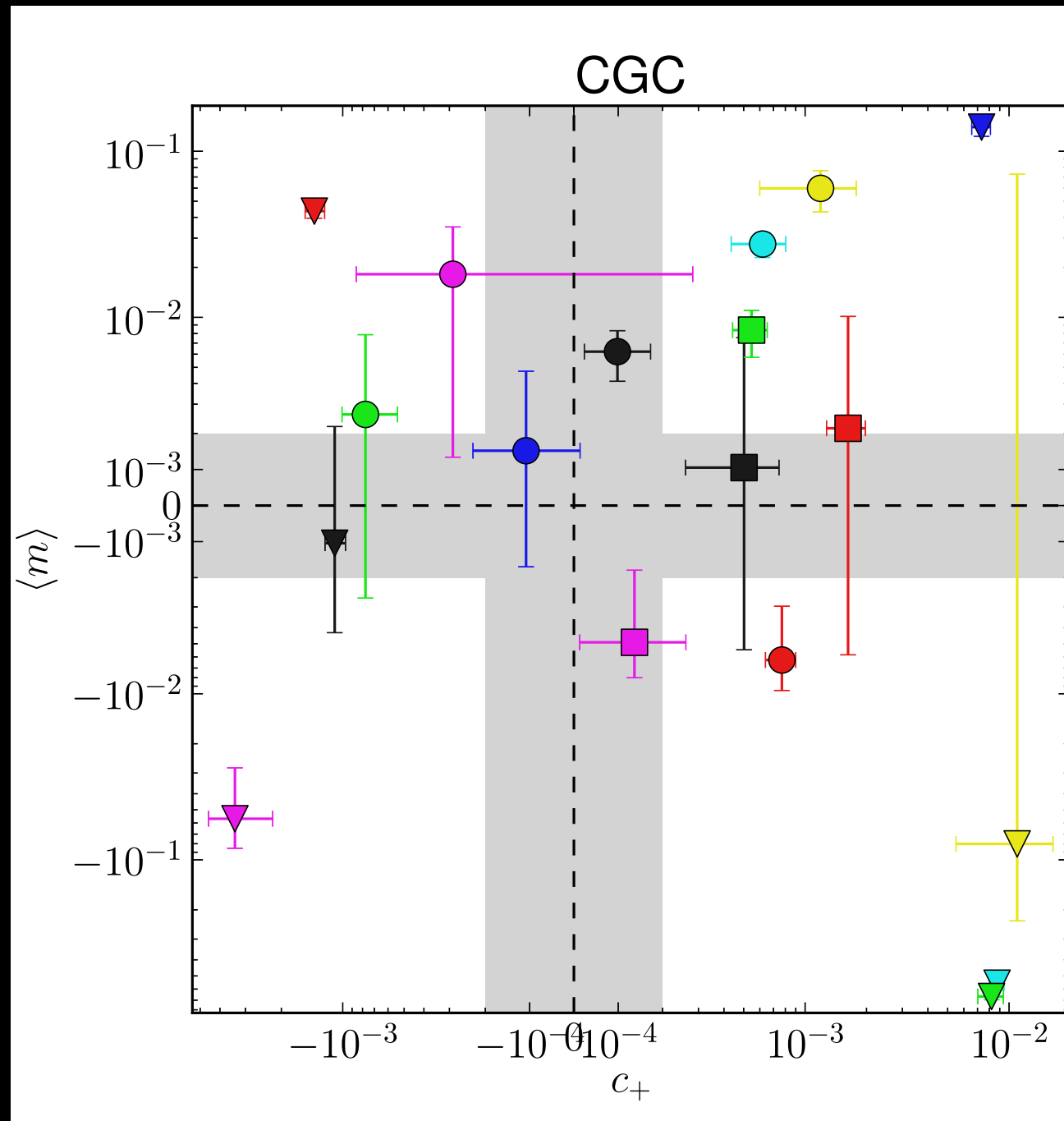
$$g = P_g^{-1} \left( e^{\text{obs}} - \frac{P^{sm}}{P^{sm*}} e^* \right)$$

**This doesn't seem that bad.**



# Mandelbaum et al. 2014

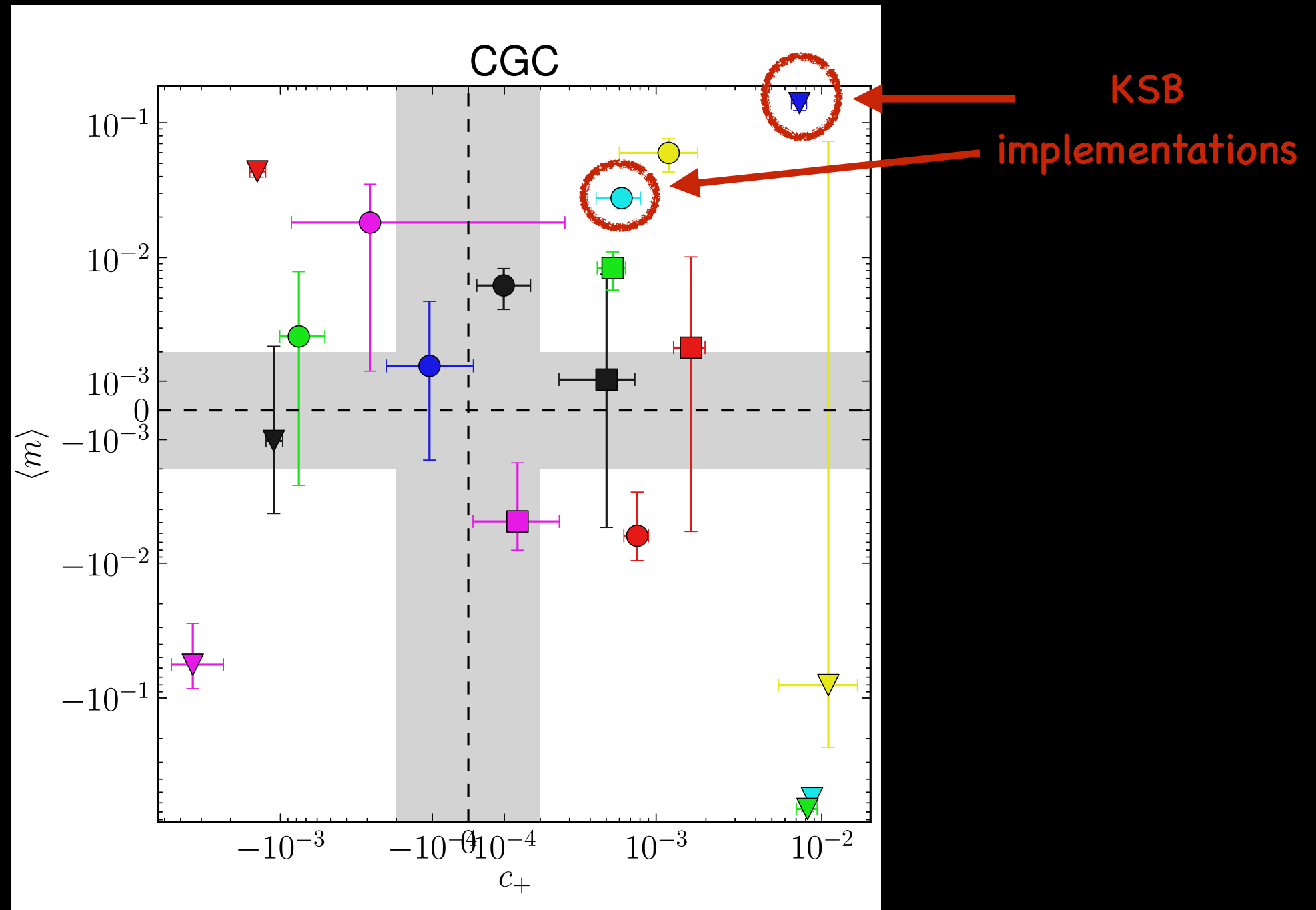
## GREAT3 Shear Calibration Community Challenge



**Alas, still broad dissensus in lensing results.**

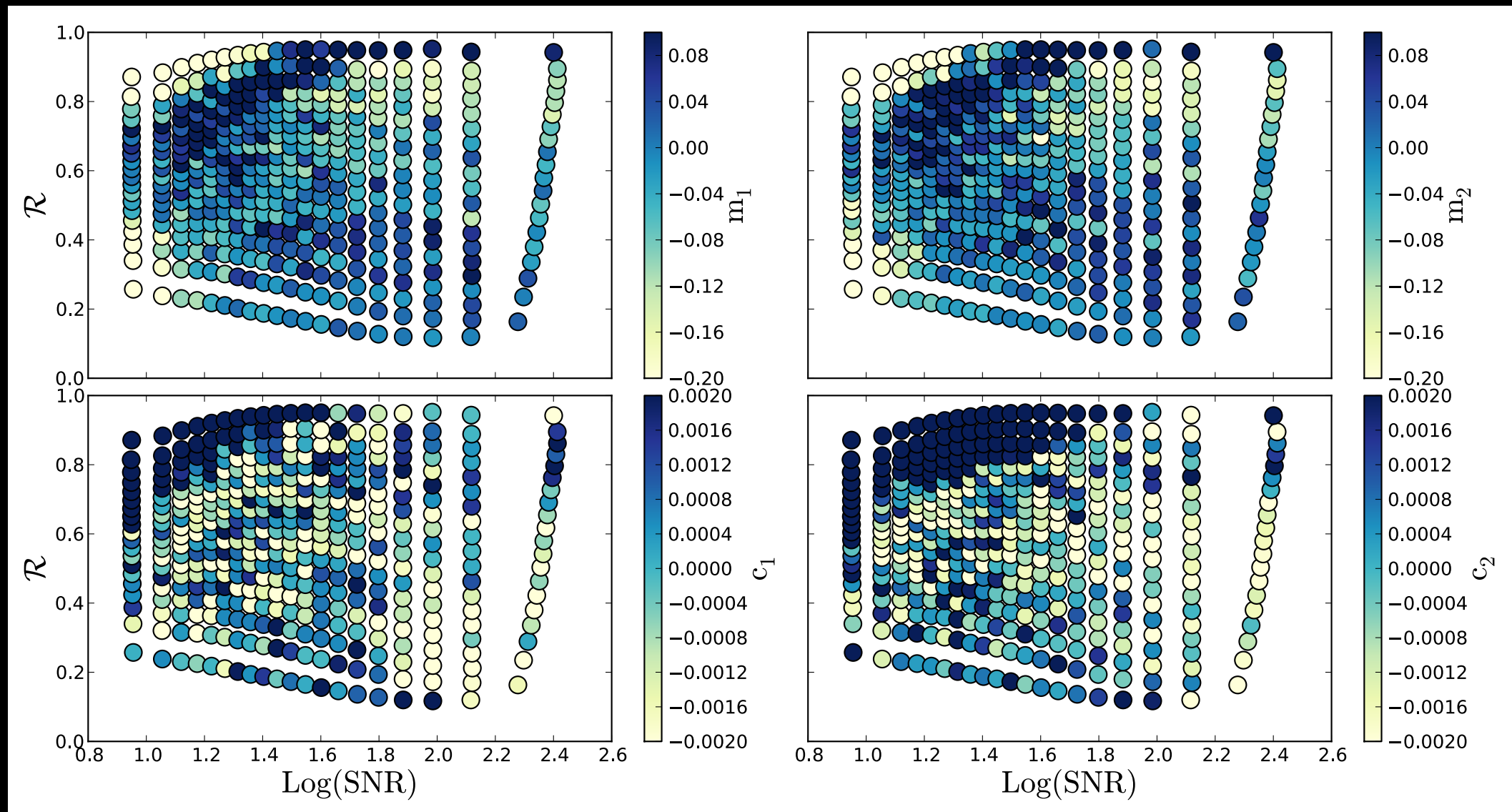
# Mandelbaum et al. 2014

## GREAT3 Shear Calibration Community Challenge

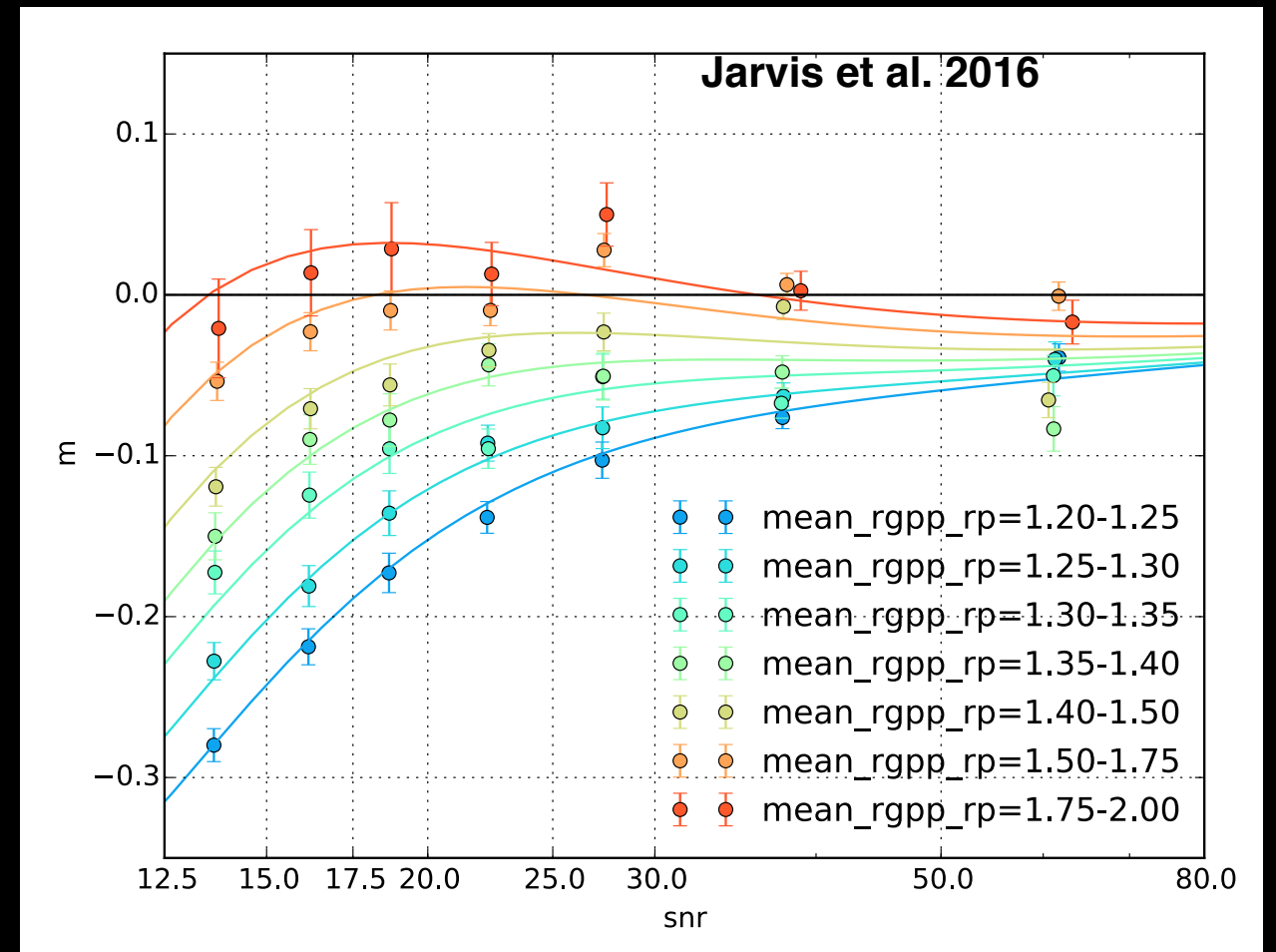
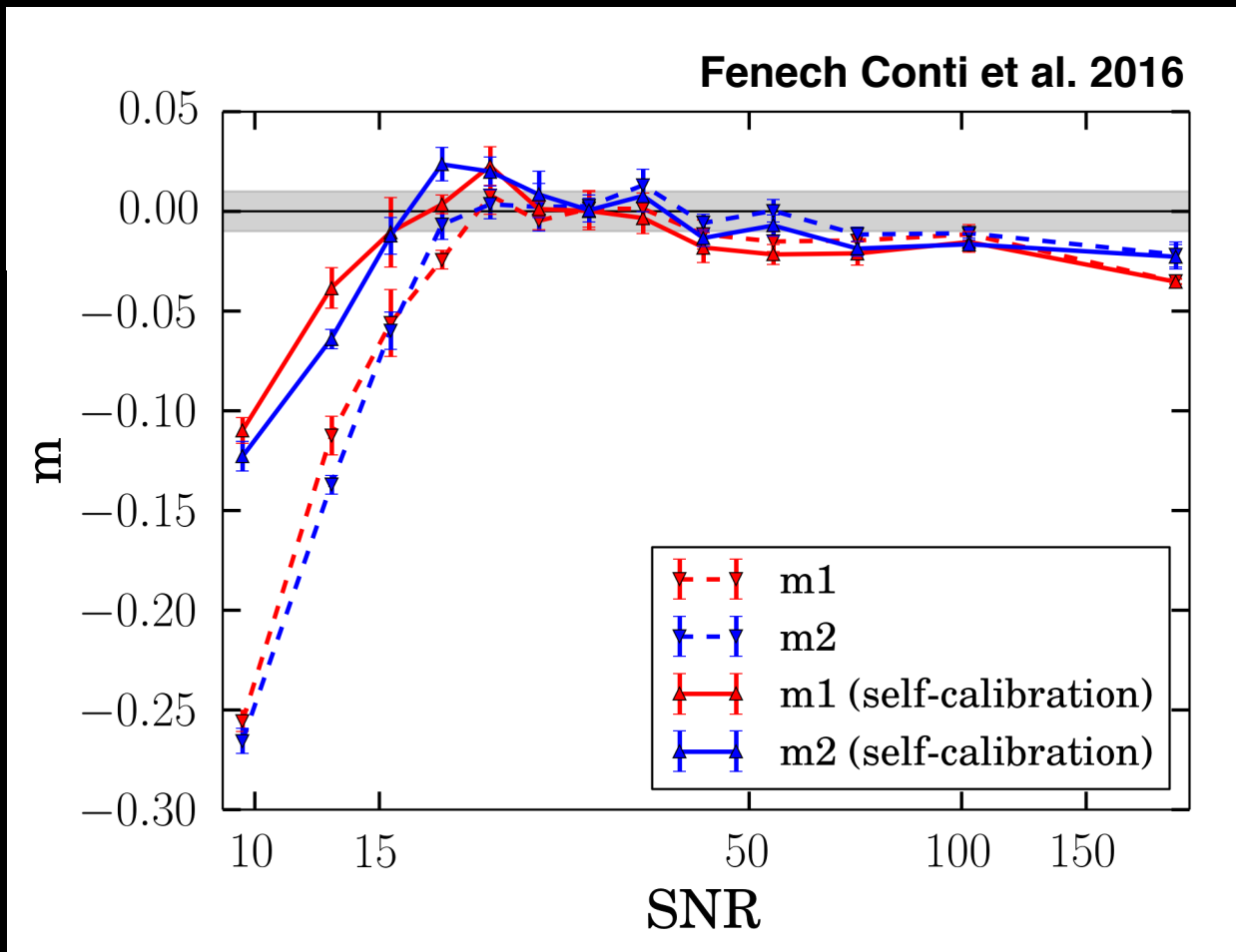


**Alas, still broad dissensus in lensing results.**

# Shear measurement biases have complex dependencies on galaxy properties.



# At low signal-to-noise, most estimators are biased.



The size and direction of these biases depends greatly on the details, including **sub-threshold** galaxy population

# What's going on?

- Images seem easy; you have an intuition that getting an 'ellipticity' from a 'galaxy' should be simple
- Analysis procedure seems 'hard', lots of details, thresholds, and nonlinear transformations.
- *“How would this image be different with more shear”* **is easier** than *“How would this measurement be different with more shear.”*

**We will construct counterfactual images.**

$$I'(\mathbf{x}|\mathbf{g}) = P * (\hat{\mathbf{S}}_{\mathbf{g}}G)$$



**We will construct counterfactual images.**

$$I'(\mathbf{x}|\mathbf{g}) = P * (\hat{\mathbf{S}}_{\mathbf{g}}G)$$

$$I'(x|g) = \Gamma * [\hat{\mathbf{S}}_g(P^{-1} * I)]$$

**remove the PSF, shear, and add a new PSF**

**We will construct counterfactual images.**

$$I'(\mathbf{x}|\mathbf{g}) = P * (\hat{\mathbf{S}}_{\mathbf{g}}G)$$

$$I'(x|g) = \Gamma * [\hat{\mathbf{S}}_g(P^{-1} * I)]$$



**we get to choose our final PSF**

**We will construct counterfactual images.**

$$I'(\mathbf{x}|\mathbf{g}) = P * (\hat{\mathbf{s}}_{\mathbf{g}}G)$$

$$I'(x|g) = \Gamma * [\hat{\mathbf{s}}_g(P^{-1} * I)]$$

$$e^+ = \hat{E} \{ I'(x|g^+) \}$$



**any ~linear measurement algorithm**

**We will construct counterfactual images.**

$$I'(\mathbf{x}|\mathbf{g}) = P * (\hat{\mathbf{s}}_{\mathbf{g}}G)$$

$$I'(x|g) = \Gamma * [\hat{s}_g(P^{-1} * I)]$$

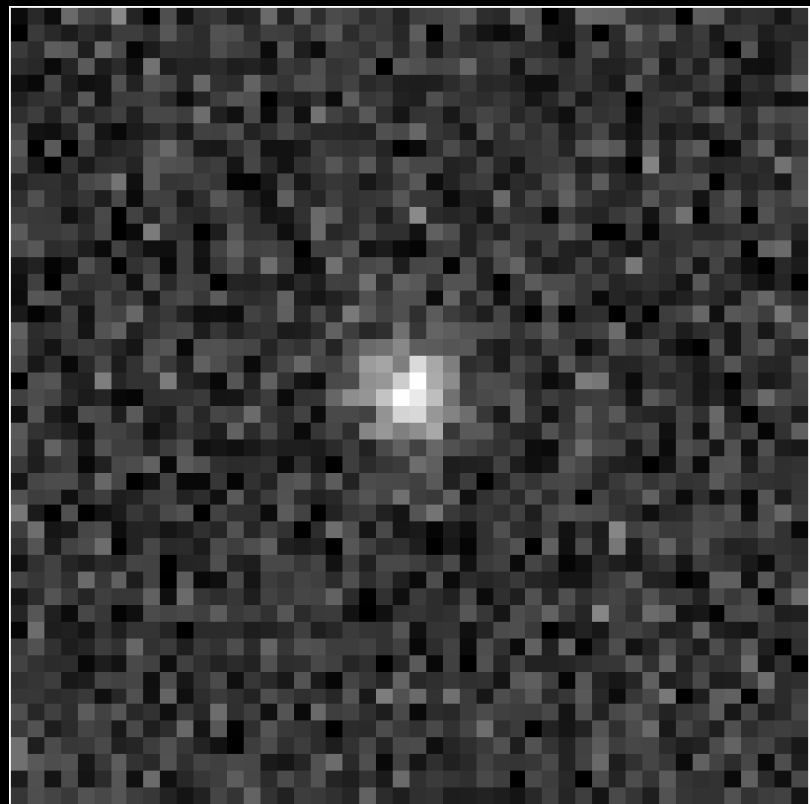
$$e^+ = \hat{E} \{ I'(x|g^+) \}$$

$$1 + m = \frac{e^+ - e^-}{2\Delta g}$$



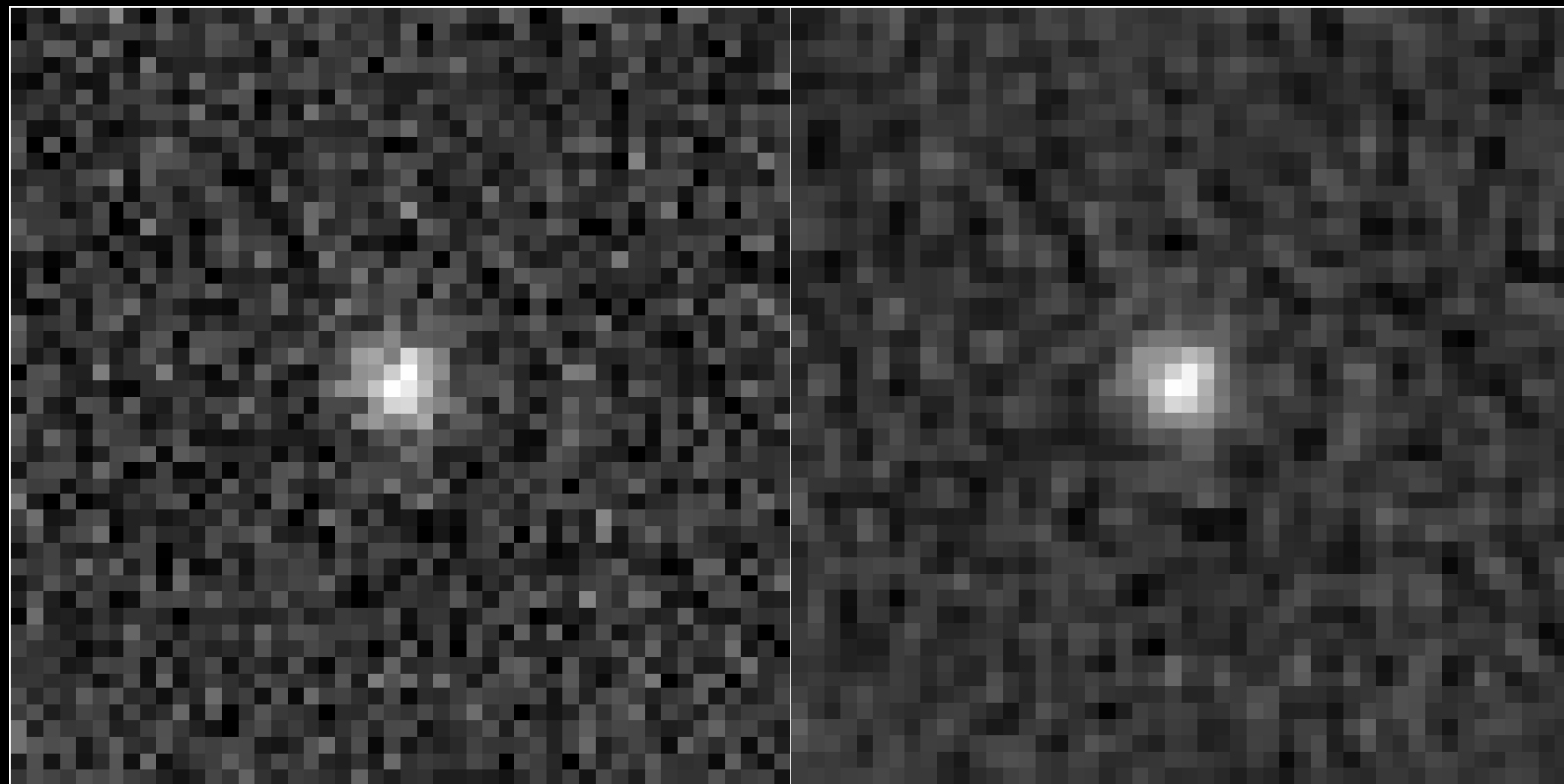
**repeated measurement on counterfactuals**

**This is what it looks like in practice.**



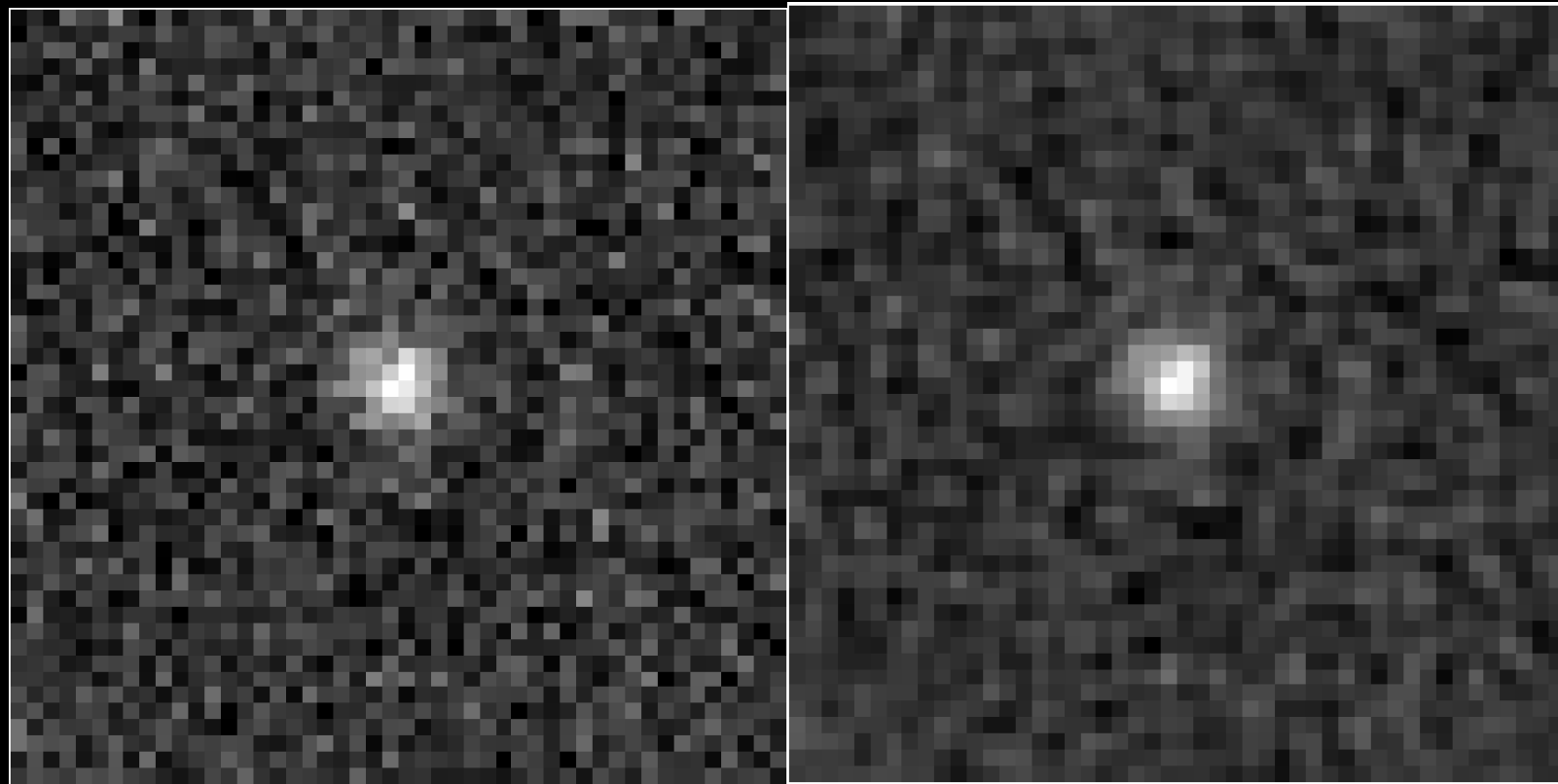
**original data**

**This is what it looks like in practice.**



**sheared, reconvolved  
(1% shear)**

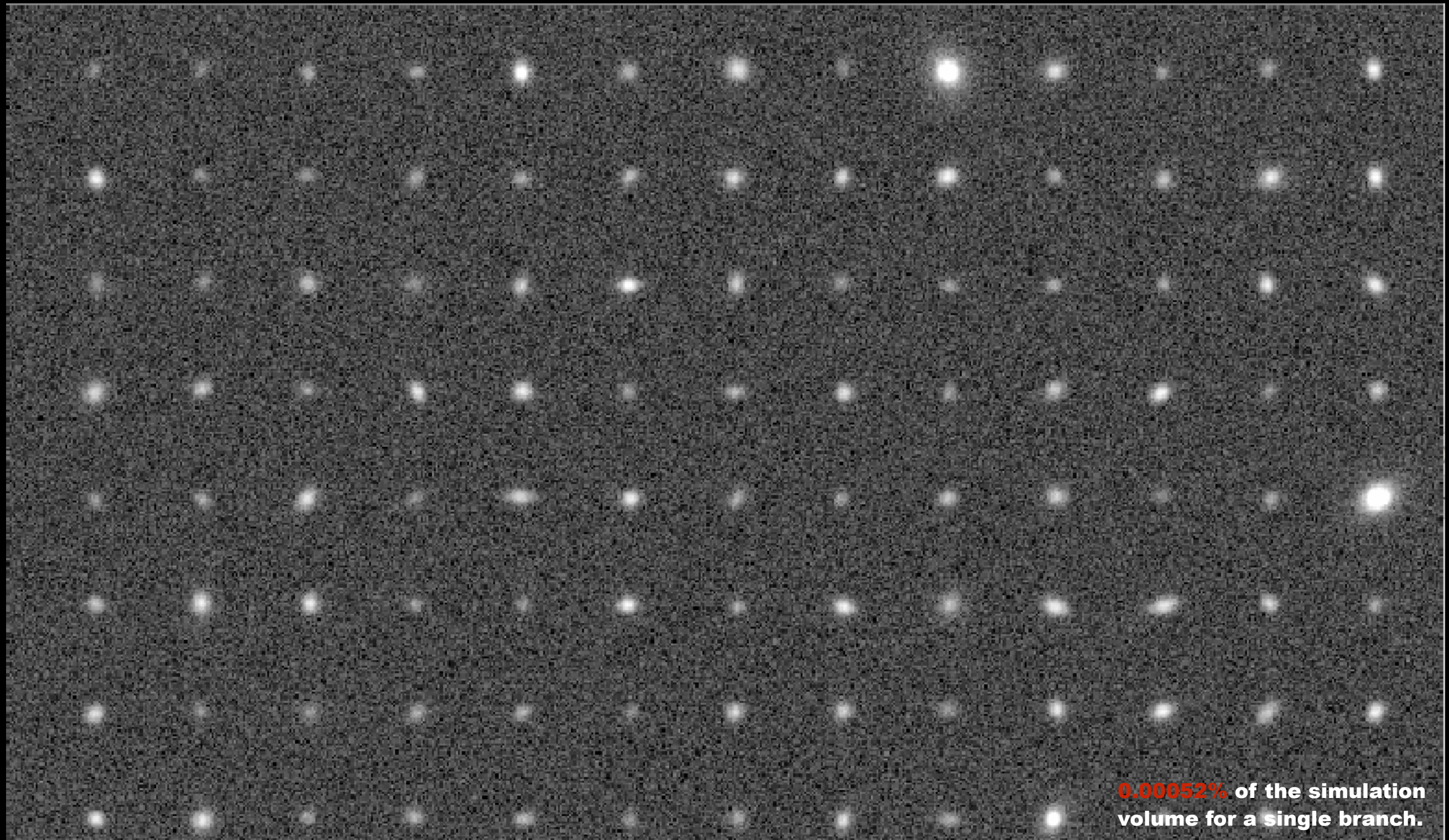
# Make measurement on unsheared counterfactual with reconvolved PSF



**un**sheared, reconvolved



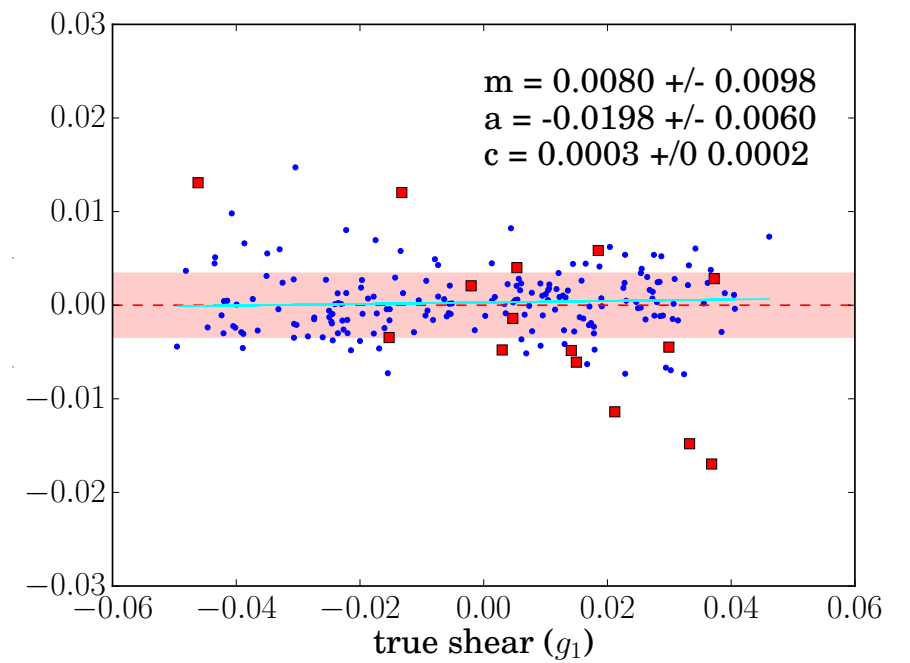
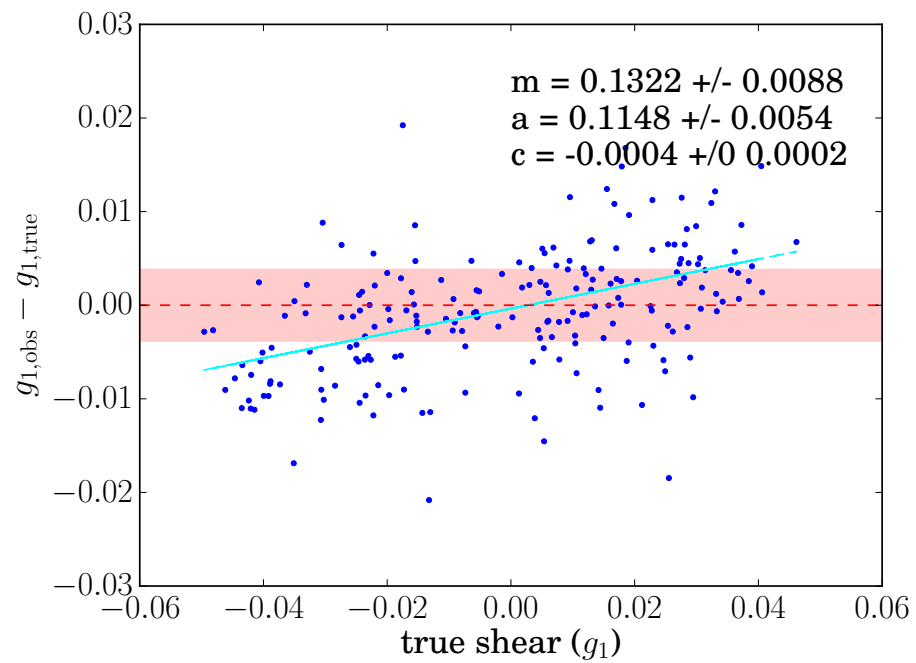
**To validate, we test on image simulations.**



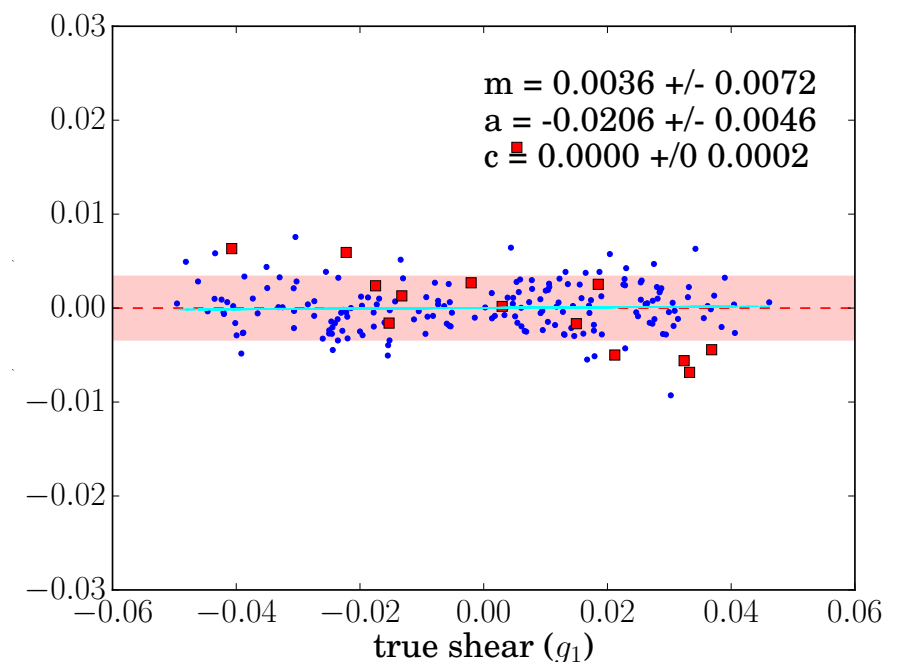
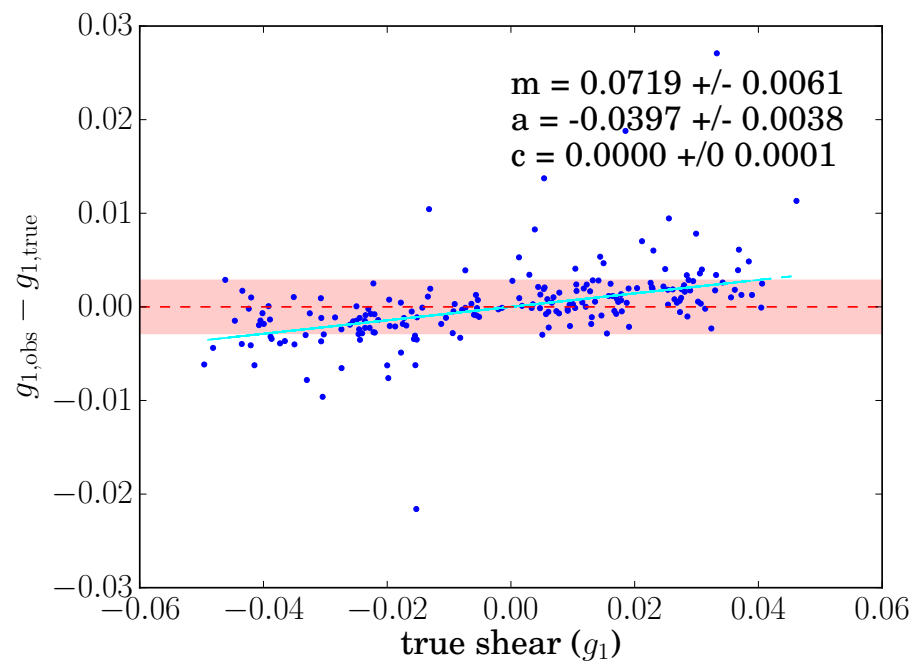
**Starting with GREAT3 analogues.**

# We wrapped Metacalibration around several measurement algorithms.

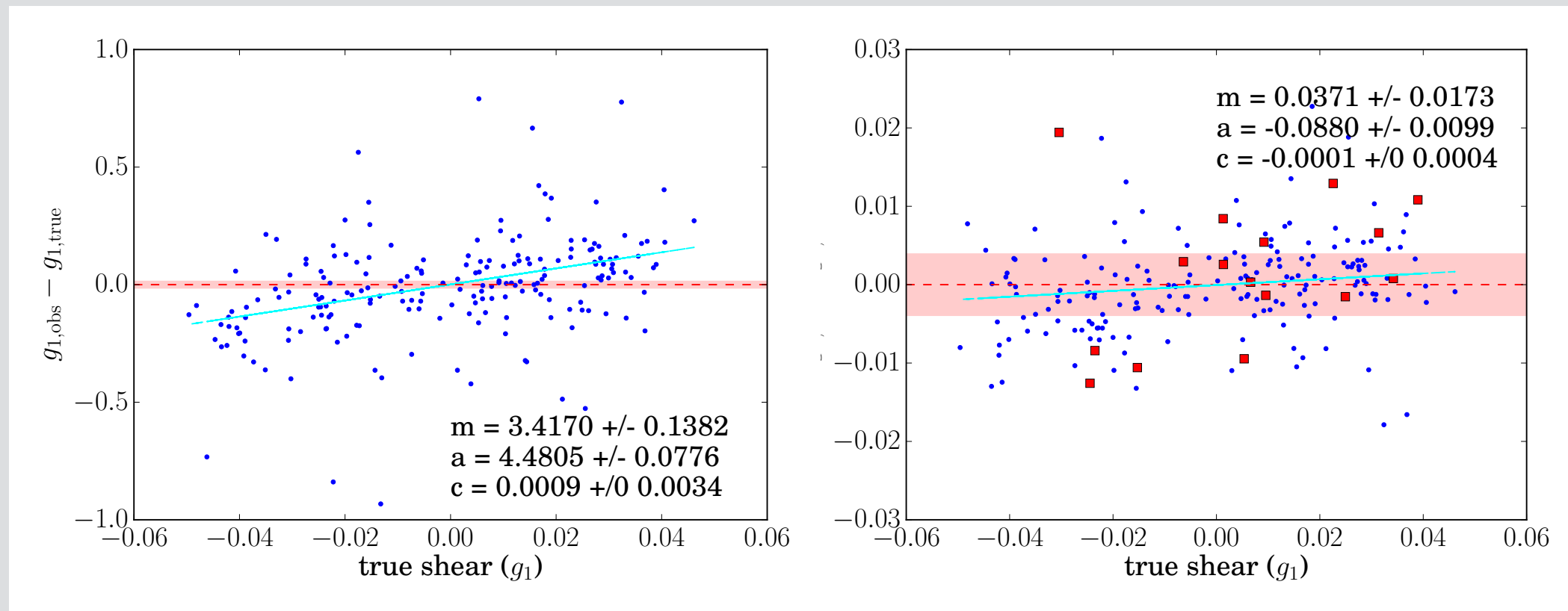
**KSB:**



**regauss:**



# We wrapped Metacalibration around several measurement algorithms.



$$M_{ij} = \frac{\int (x_i - \langle x_i \rangle)(x_j - \langle x_j \rangle) w(\mathbf{x}) I(\mathbf{x}) d^2 \mathbf{x}}{\int w(\mathbf{x}) I(\mathbf{x}) d^2 \mathbf{x}}$$

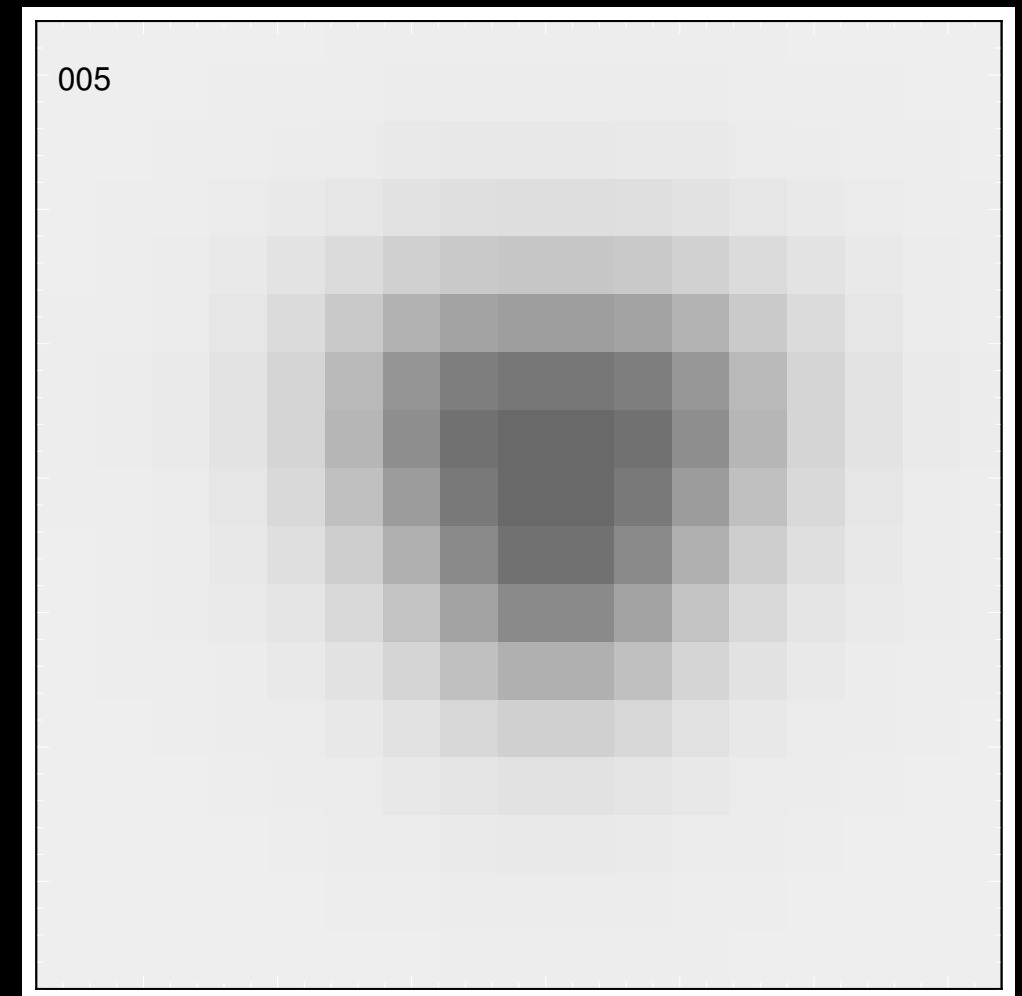
$$e_1 = \frac{M_{11} - M_{22}}{M_{11} + M_{22}}, \quad e_2 = \frac{2M_{12}}{M_{11} + M_{22}}$$

$$\hat{M}_i = (M_{11} - M_{22}, 2M_{12}).$$

...including uncorrected second moments,  
which should not work at all.

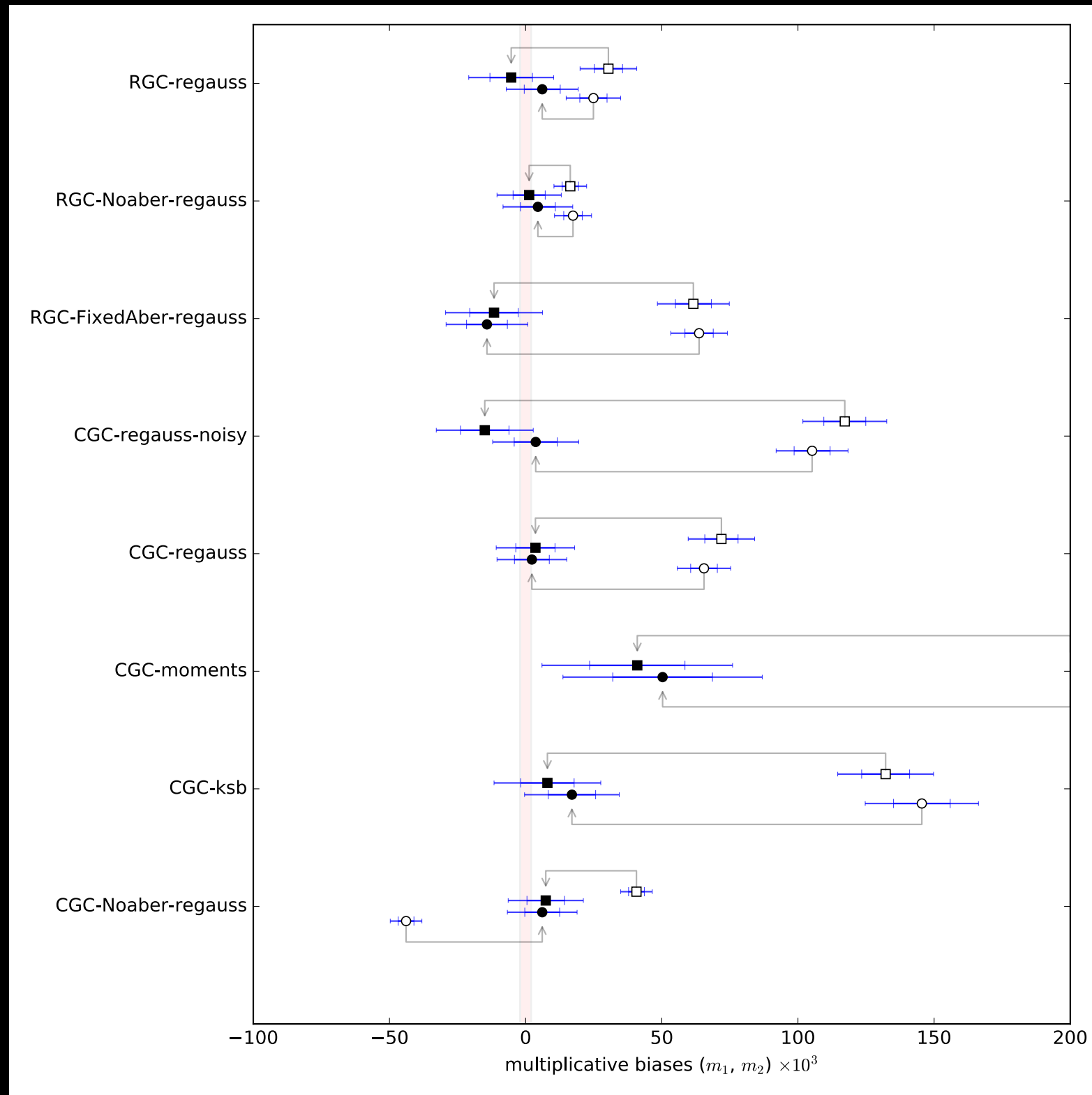
# We ran many simulations, varying the complexity

- real galaxy morphology
- heterogeneous PSF
- increased noise
- large optical aberrations
- flawed measurement algorithms

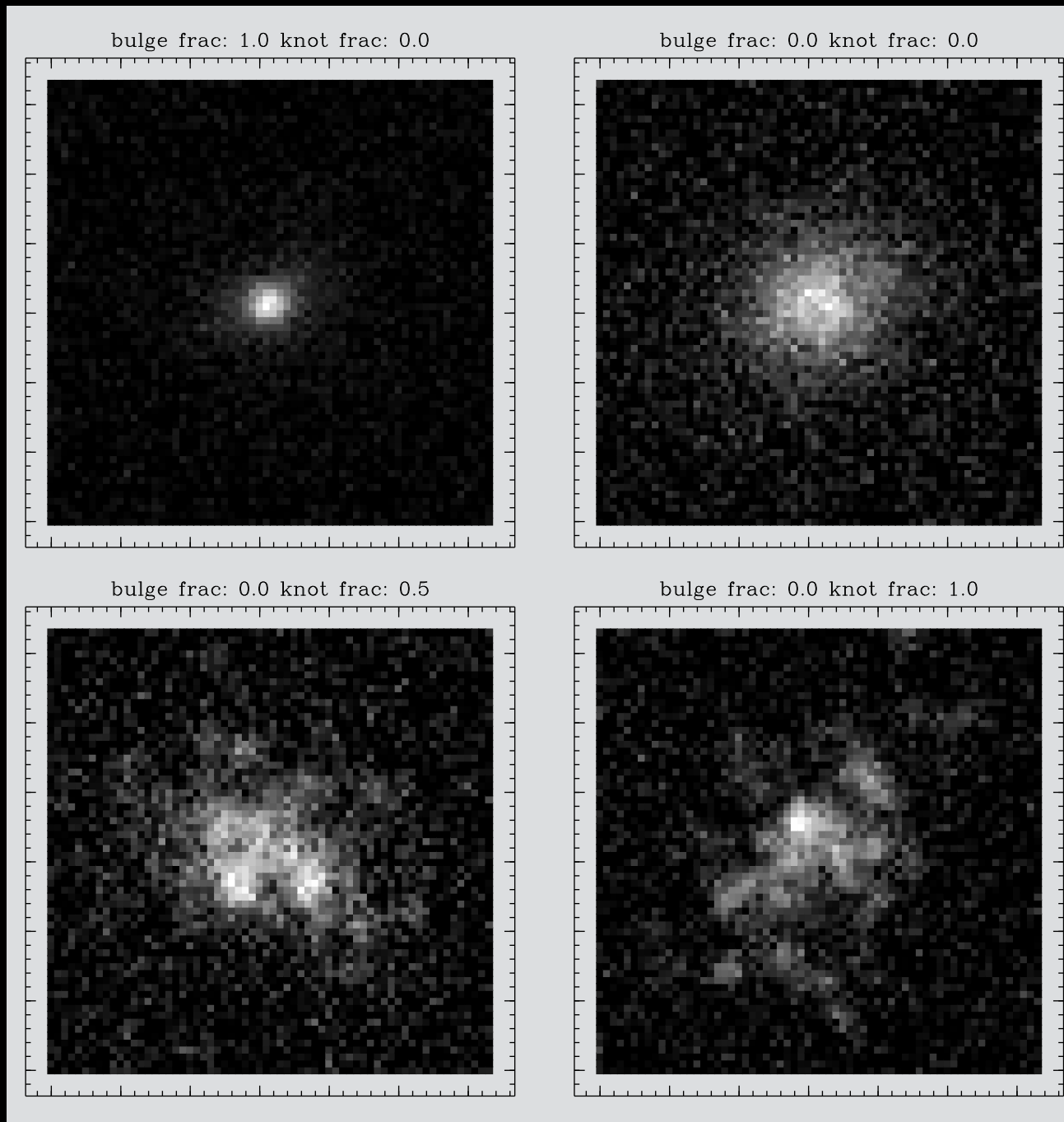


Huff & Mandelbaum 2017

# Where the algorithms are correctable, MetaCal calibrates them.



# Parallel collaboration with Erin Sheldon: pushing Metacalibration's limits



## BDK+ Simulations:

Much larger simulation volume ( $5 \times 10^9$ )  
Bulge+Disk+knots  
realistic size/flux distribution (COSMOS)  
stellar contamination  
full Dark Energy Survey PSF  
Large sub-threshold population (low S/N)

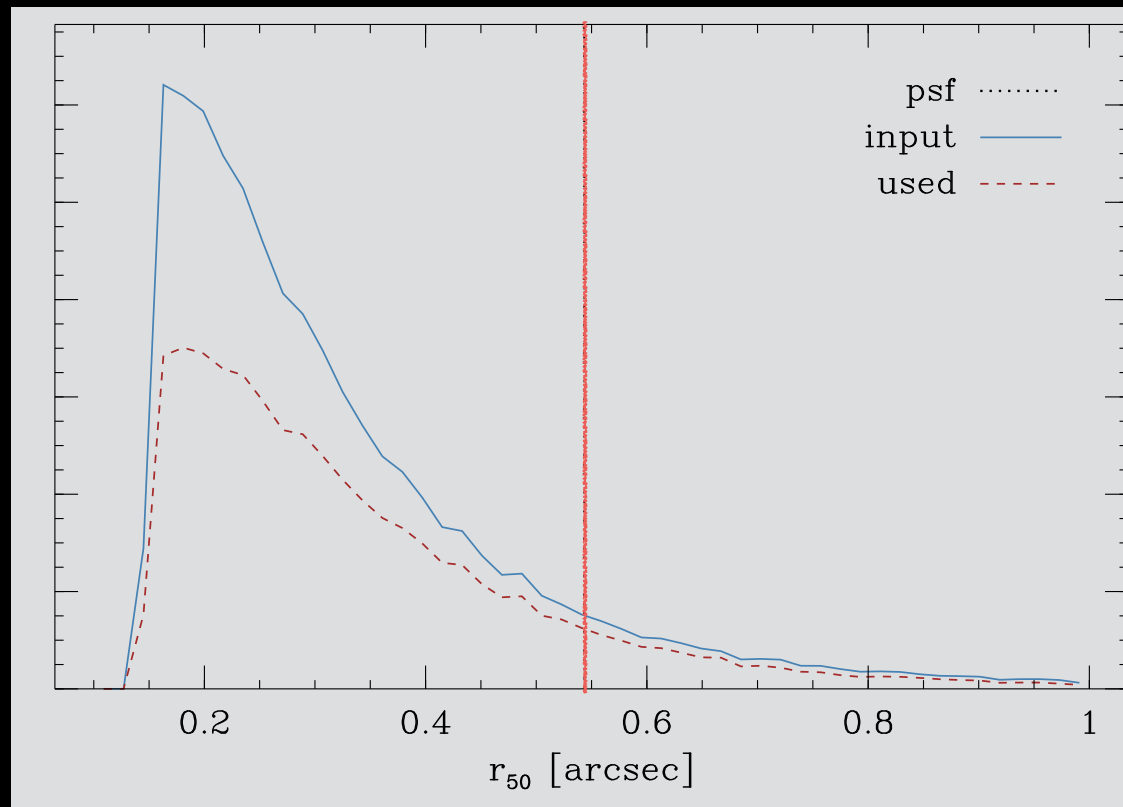
## Simplified Measurement:

fit elliptical gaussian  
no PSF correction (!!!)  
reconvolve to symmetric PSF  
add noise to symmetrize

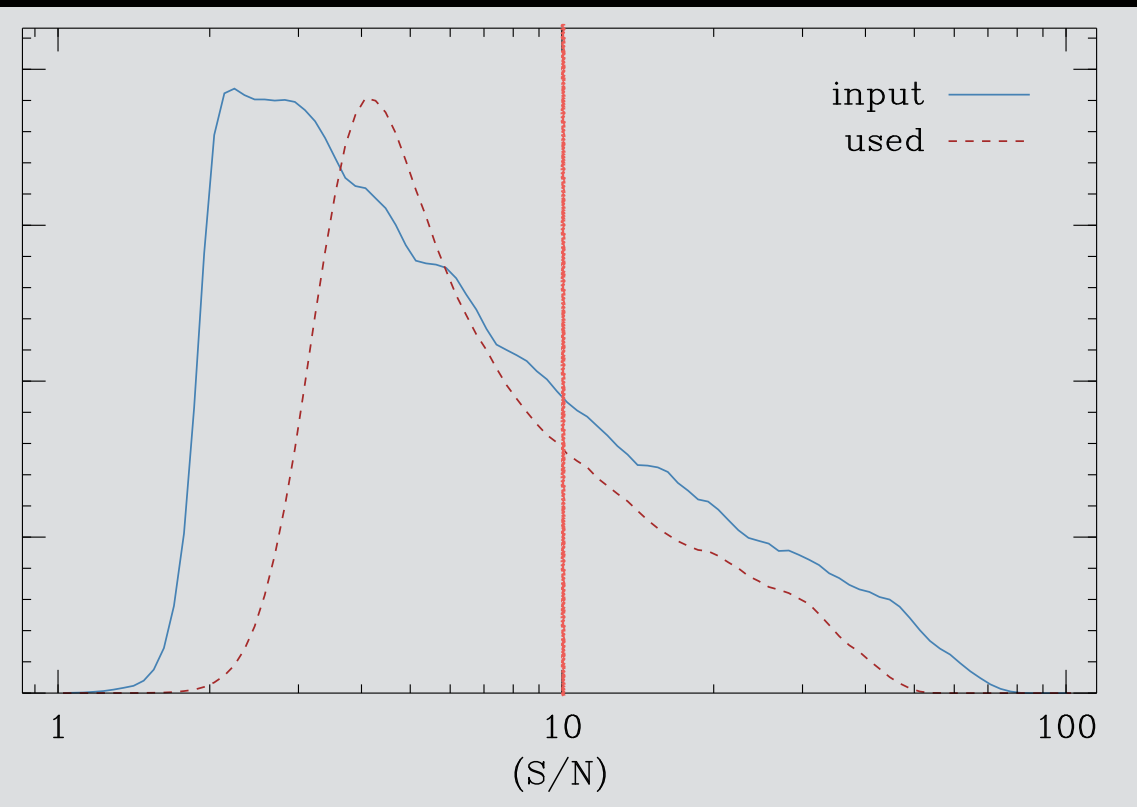


**These simulations include large sub-threshold populations, so selection effects matter.**

**PSF ( $r_{50}$ )**

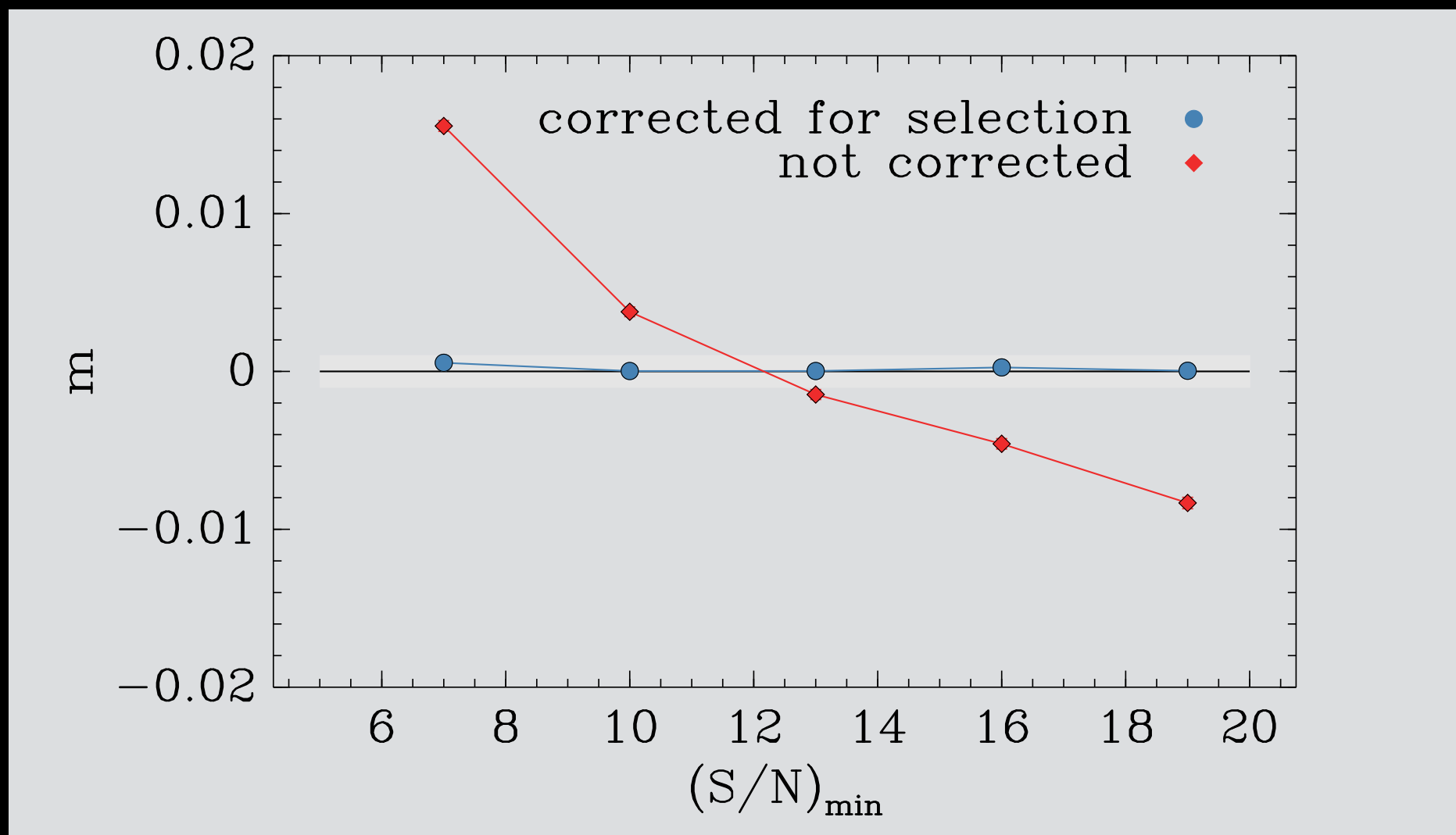


**S/N threshold**





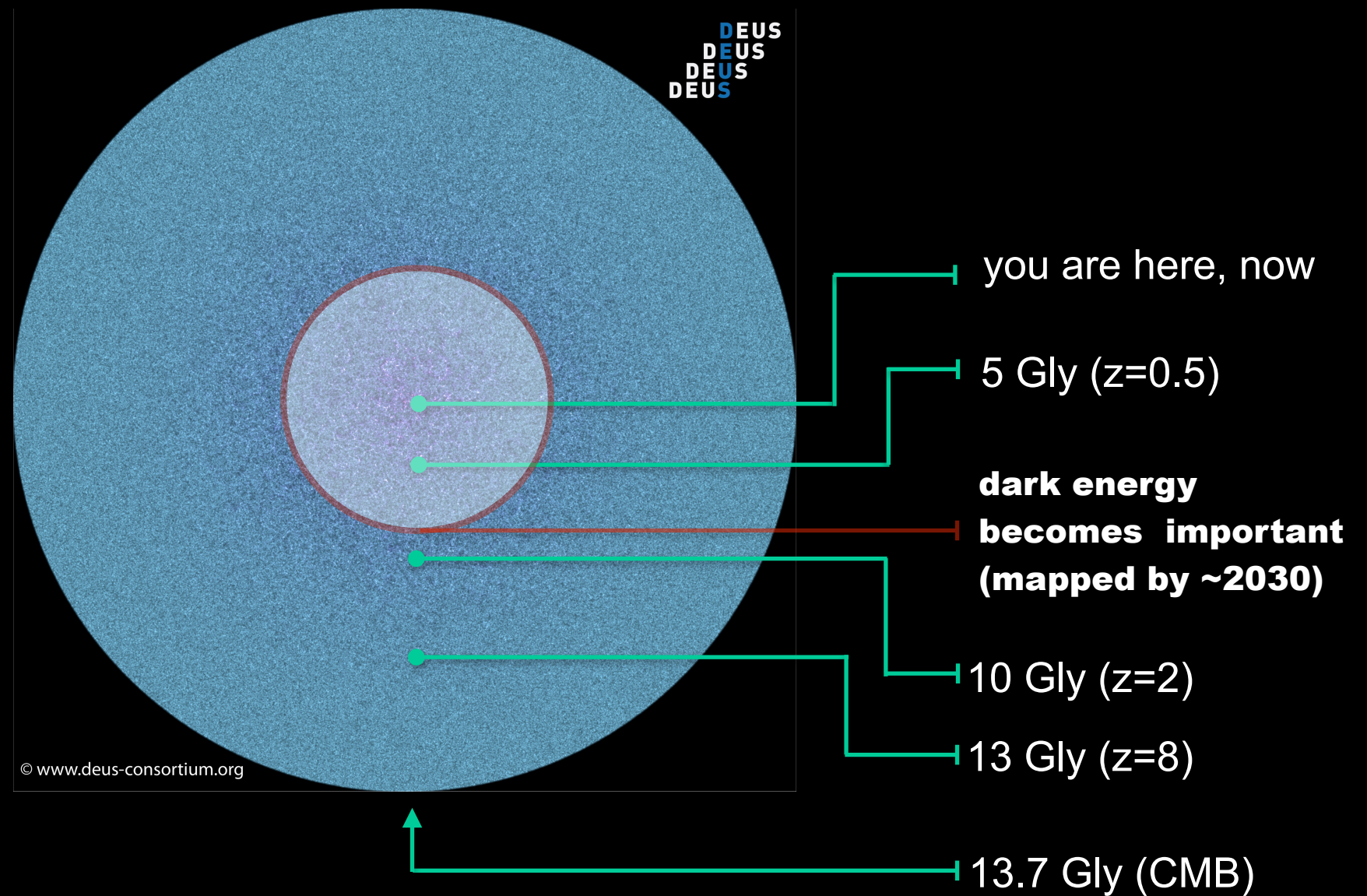
**Selection effects are large,  
but now effectively mitigated.**



**There is no evidence  
for any remaining calibration bias.**

# FUTURE PROBLEMS

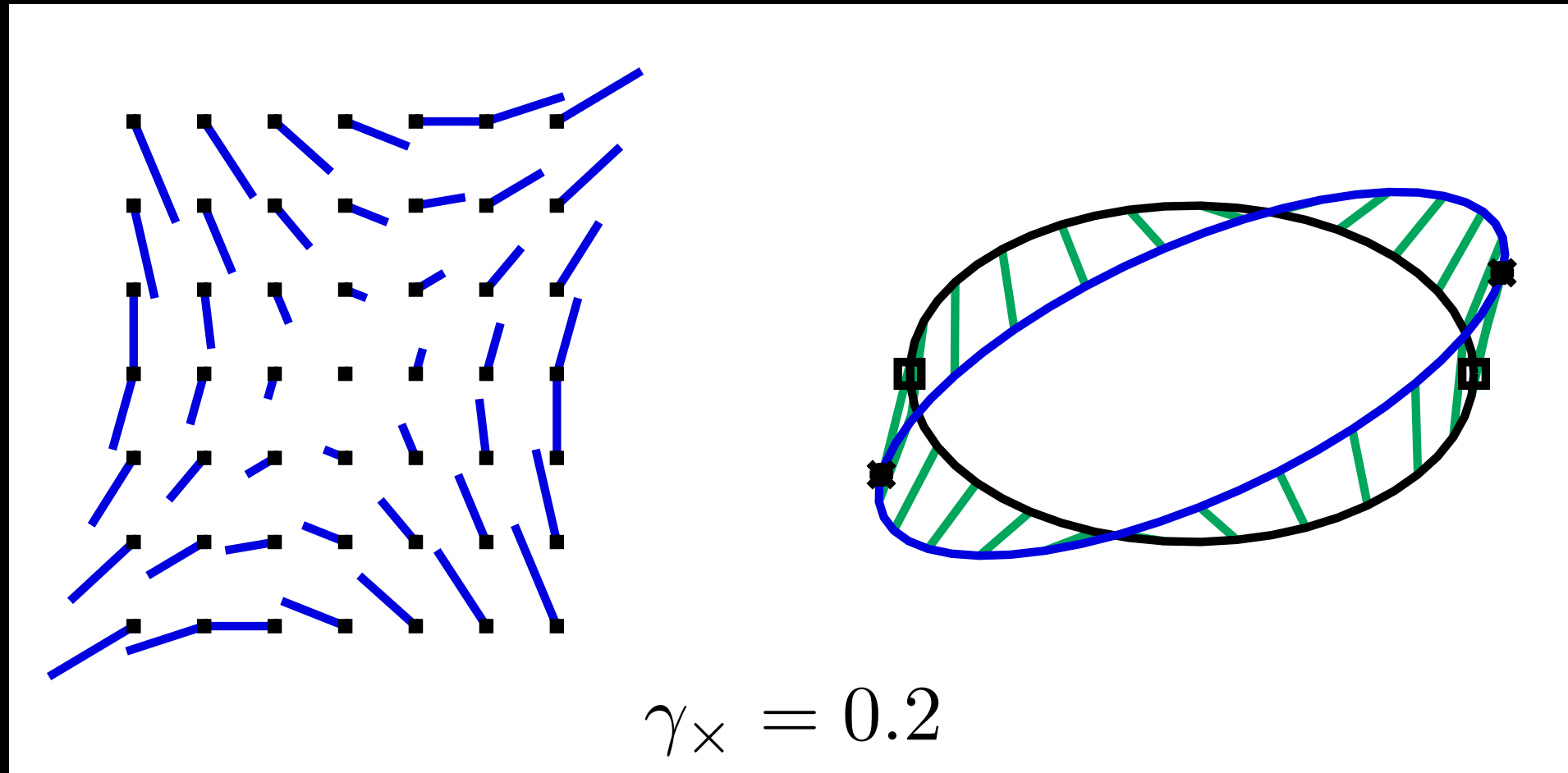
We will soon run out of universe  
for dark energy measurements.



It is unlikely that we will have solved  
everything by then.

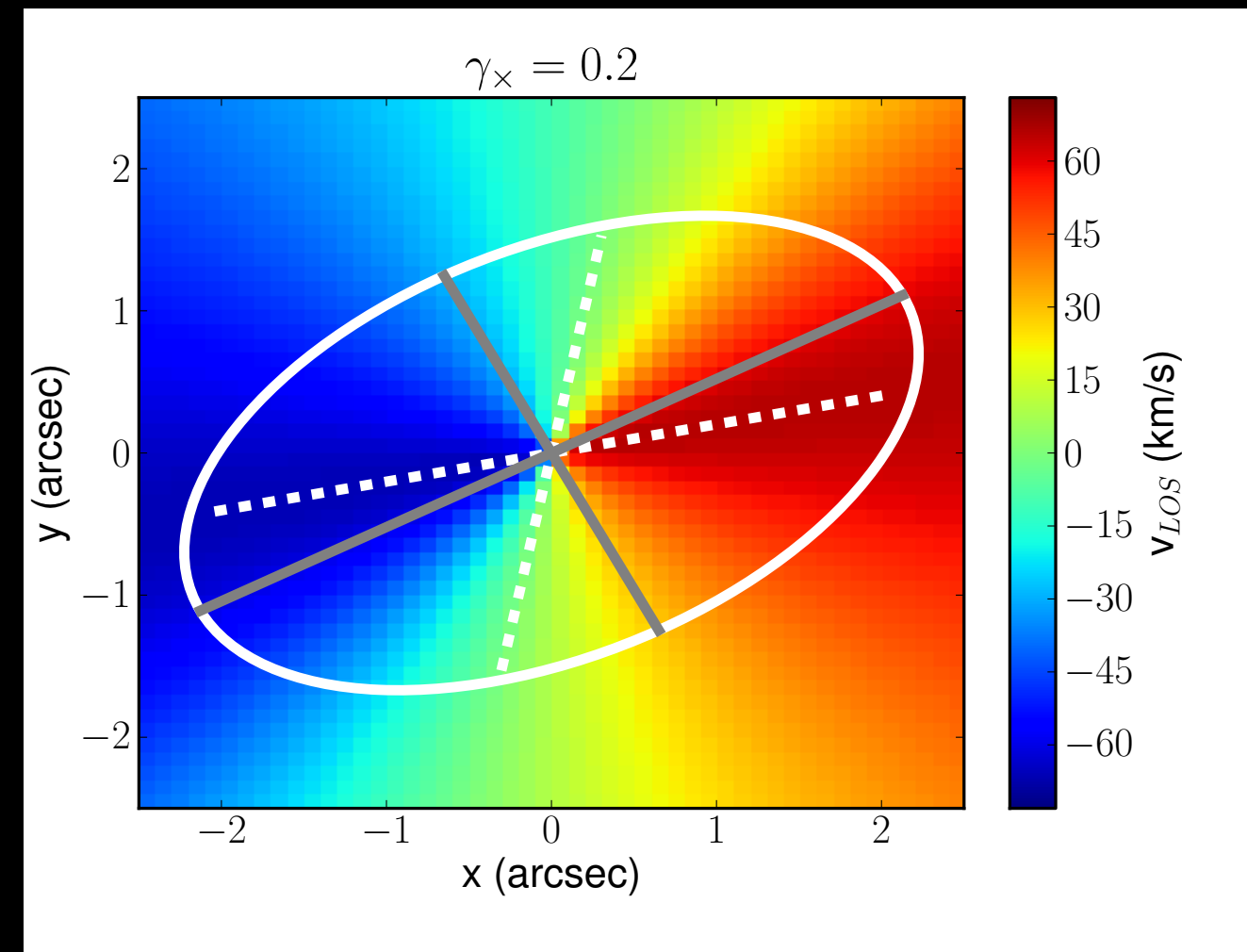
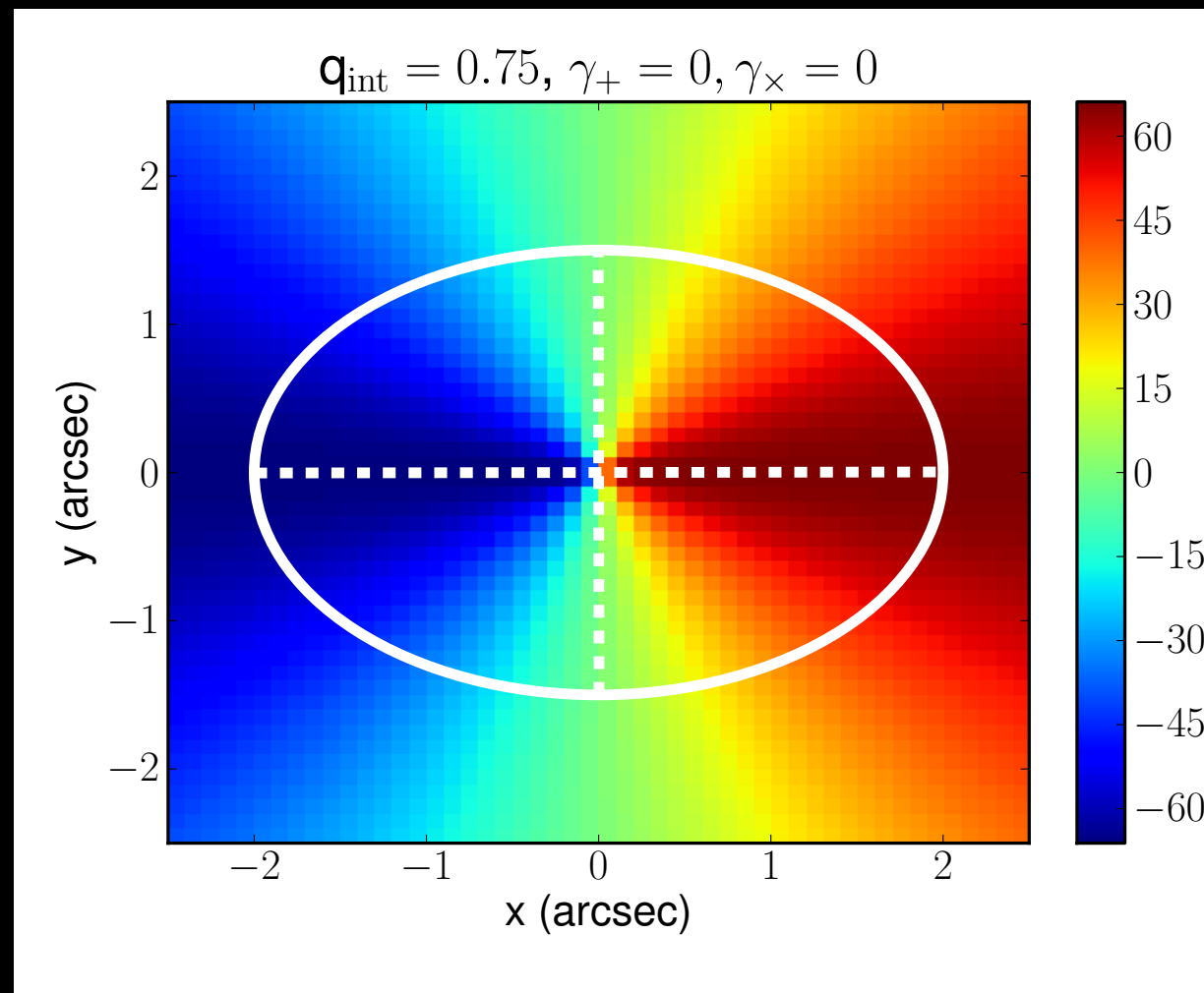
**IF WE CANNOT FIND MORE GALAXIES,  
WE NEED MORE INFORMATION PER GALAXY.**

# Shear changes the orientation of an ellipse



But shear has no solid-body rotation component.

# Lensing *mis-aligns* the kinematic and photometric axes



With spectroscopic maps, this should be detectable.

# Kinematics break degeneracy between shape and shear

image



face-on

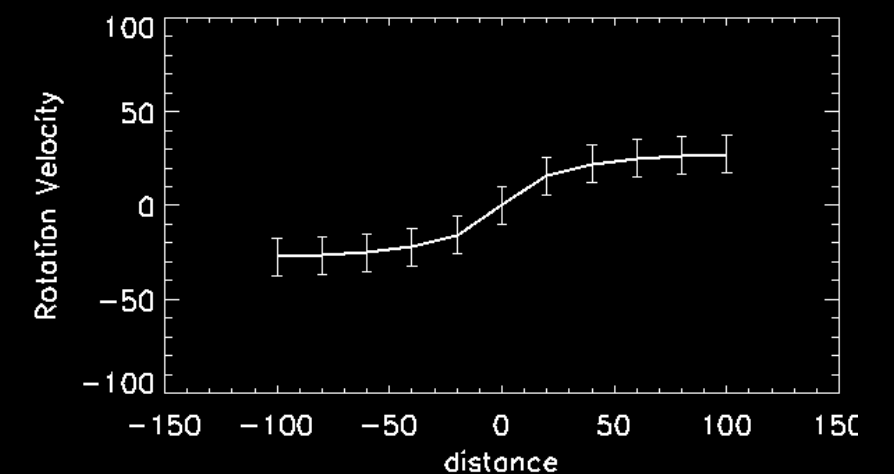
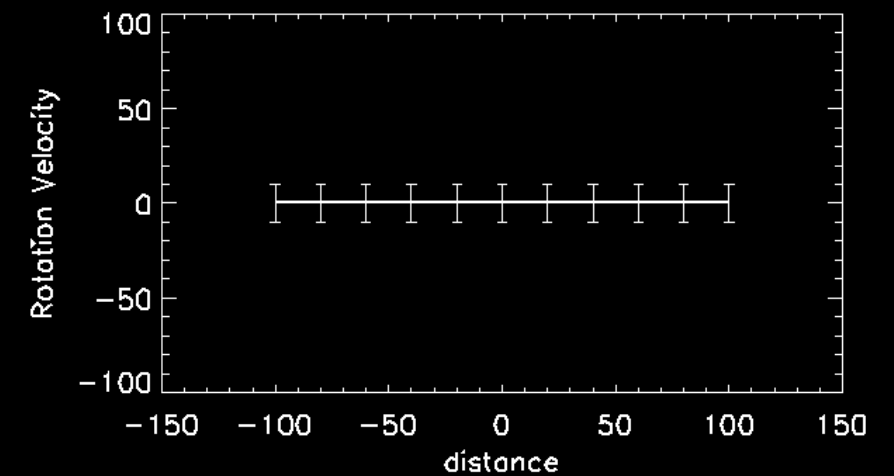
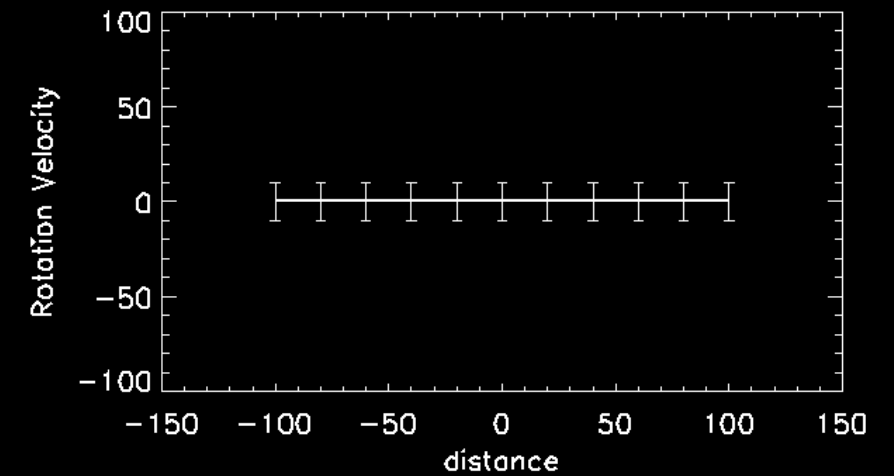


face-on, but sheared



inclined, but not sheared

rotation curve





# Consider the Tully-Fisher relation.

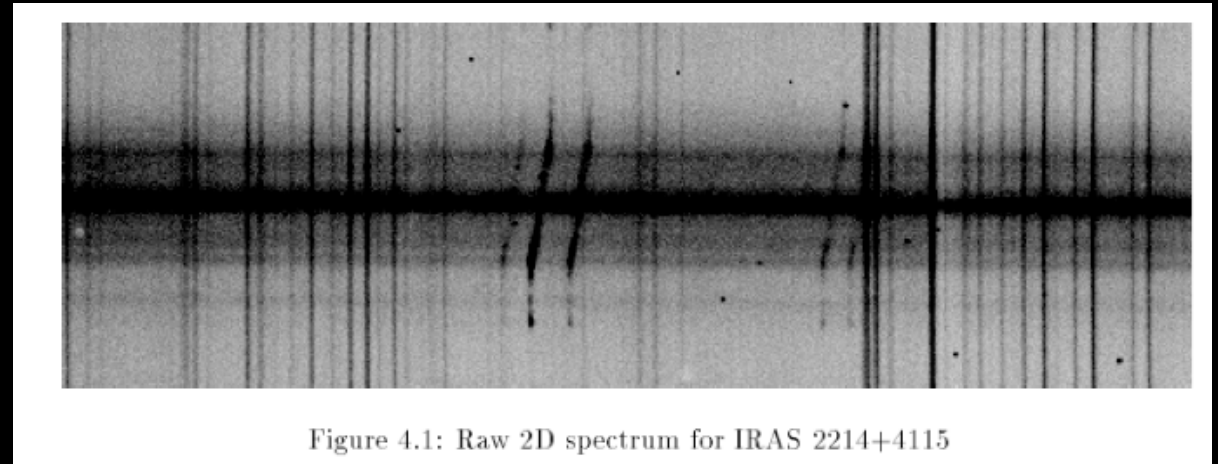
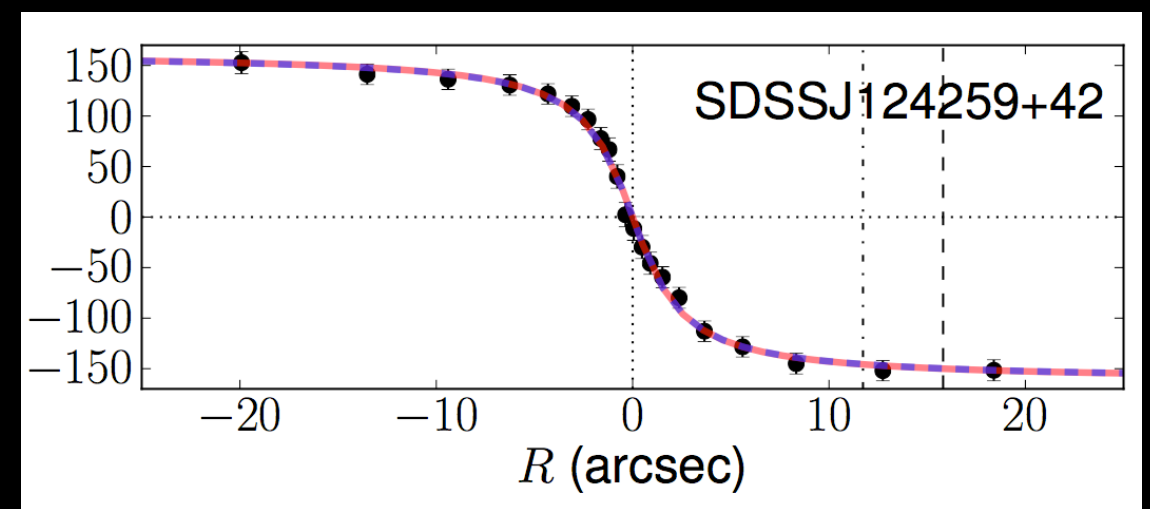
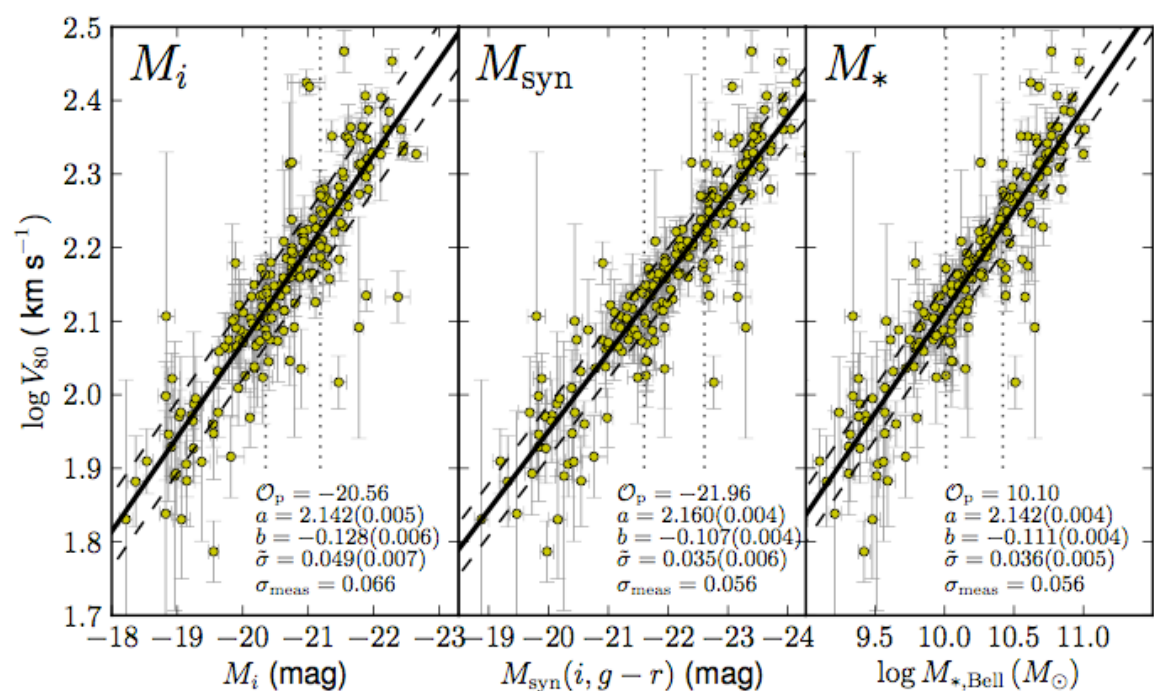


Figure 4.1: Raw 2D spectrum for IRAS 2214+4115

Schlegel (private comm.)

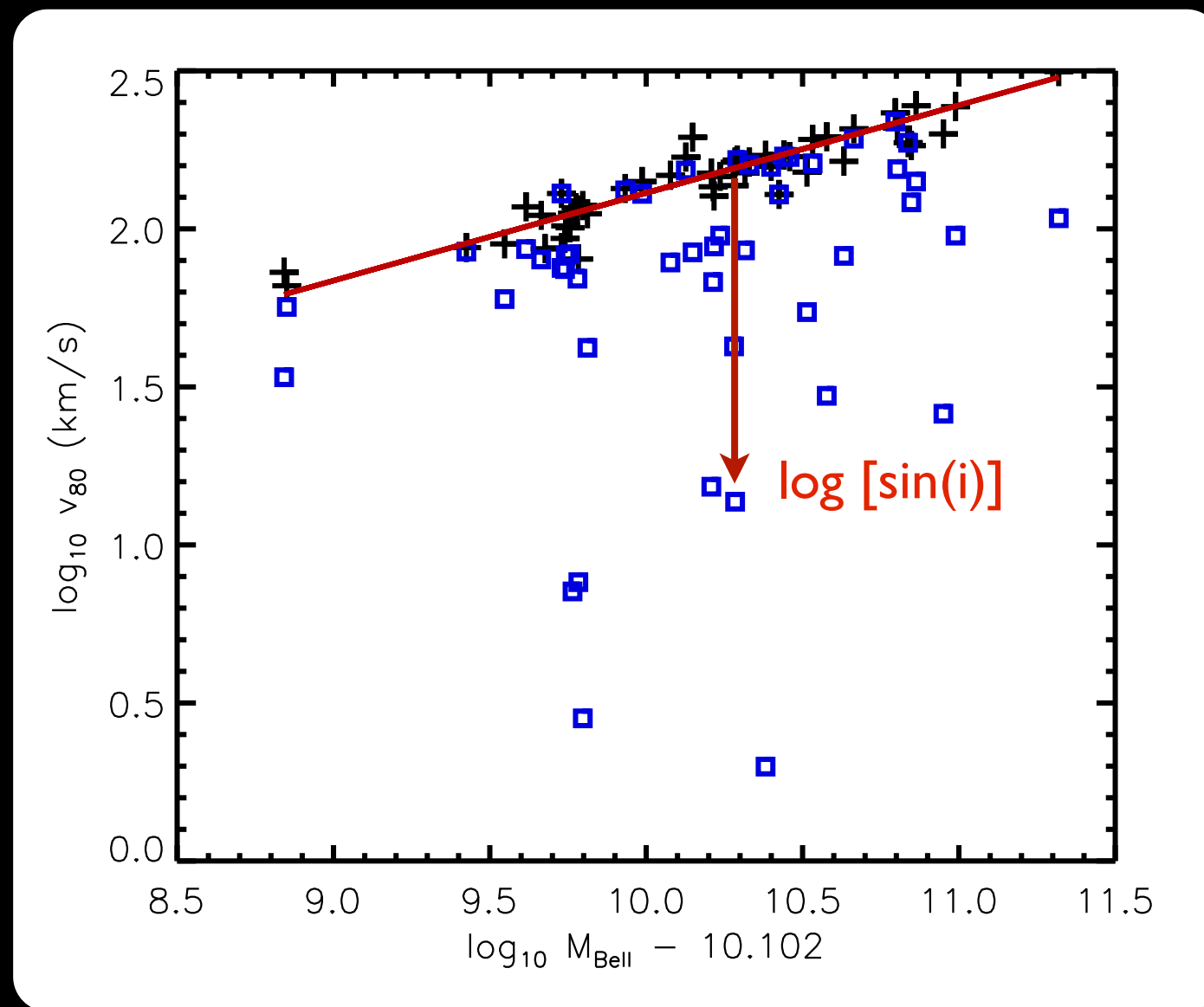


Reyes et al 2011



Reyes et al 2011

With spectroscopy, the Tully-Fisher relation tells us the inclination angle.



Blue points:  
not corrected for  
inclination

Red trendline:  
TF relation, which we  
treat as given

For a disk,  $\sin(i)$  tells us what ellipticity we should measure in the absence of lensing.

Shear messes up the inclination correction.

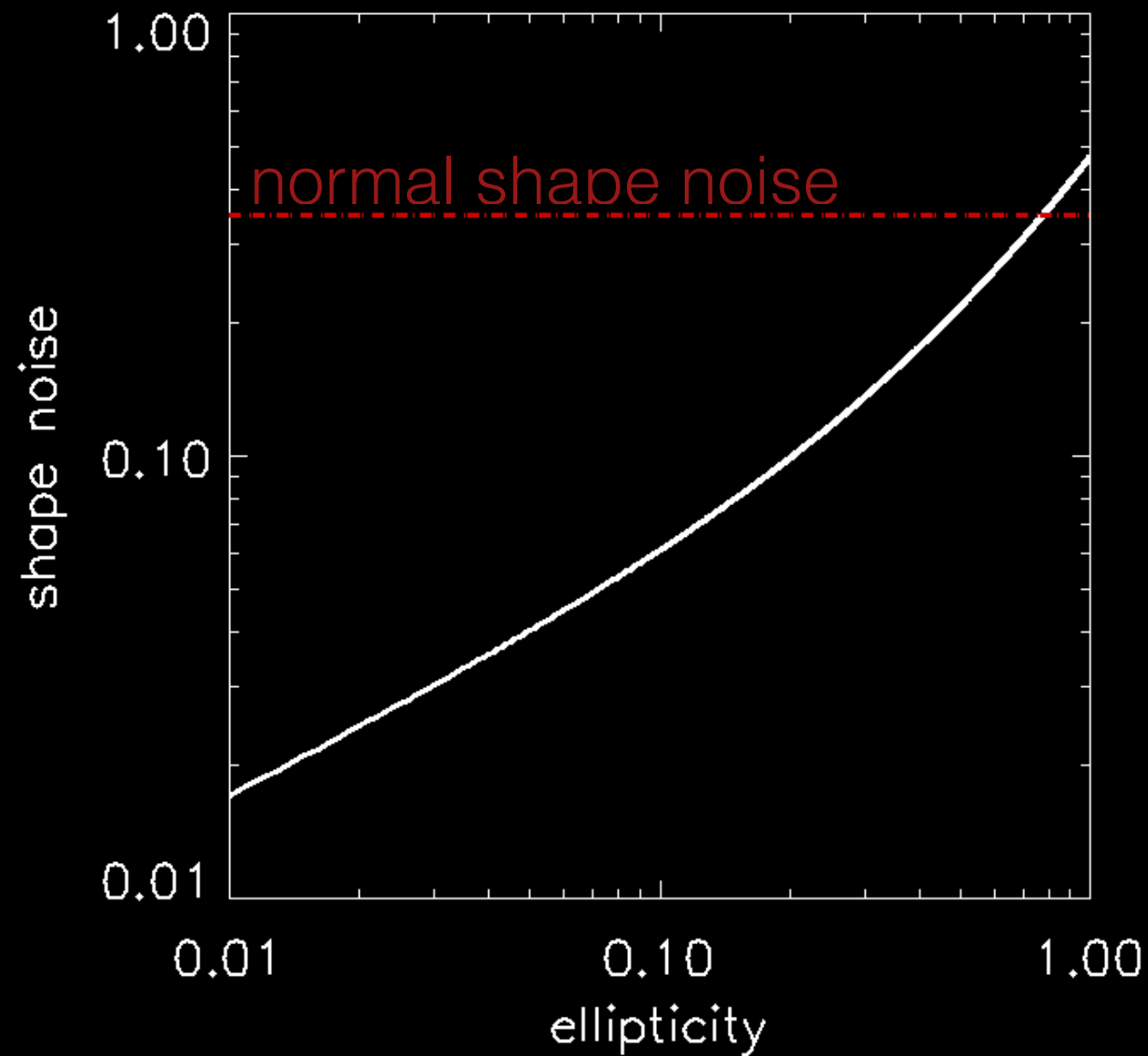
Tully-Fisher:  $v_{\text{obs}} = v_{\text{TF}} \sin(i) + \sigma_{\text{TF}}$

For a disk:  $\sin(i) = \left( \frac{2e}{1+e} \right)^{\frac{1}{2}}$

The effect of a shear:  $e \mapsto e + \gamma$

$$\sin(i)|_{\gamma} = \sin(i)|_{\gamma=0} + \frac{\gamma}{2\sqrt{e(1+e)^3}}$$

The reduction in shape noise can be very large...



...For face-on disks, factors of  $\sim 10$ .

For this level of per-galaxy shape noise:

$$\text{Shape noise: } \propto \frac{\sigma_e}{\sqrt{n_{\text{gal}}}}$$

$$\begin{aligned} \text{For LSST: } \quad n_{\text{gal}} &\approx 25 \text{ gal arcmin}^{-2} \\ \sigma_e &\approx 0.2 \end{aligned}$$

For kinematic lensing, equivalent shape noise with:

$$\begin{aligned} \sigma_e &\approx 0.025 \\ n_{\text{gal}} &\approx .25 \text{ gal arcmin}^{-2} \end{aligned}$$

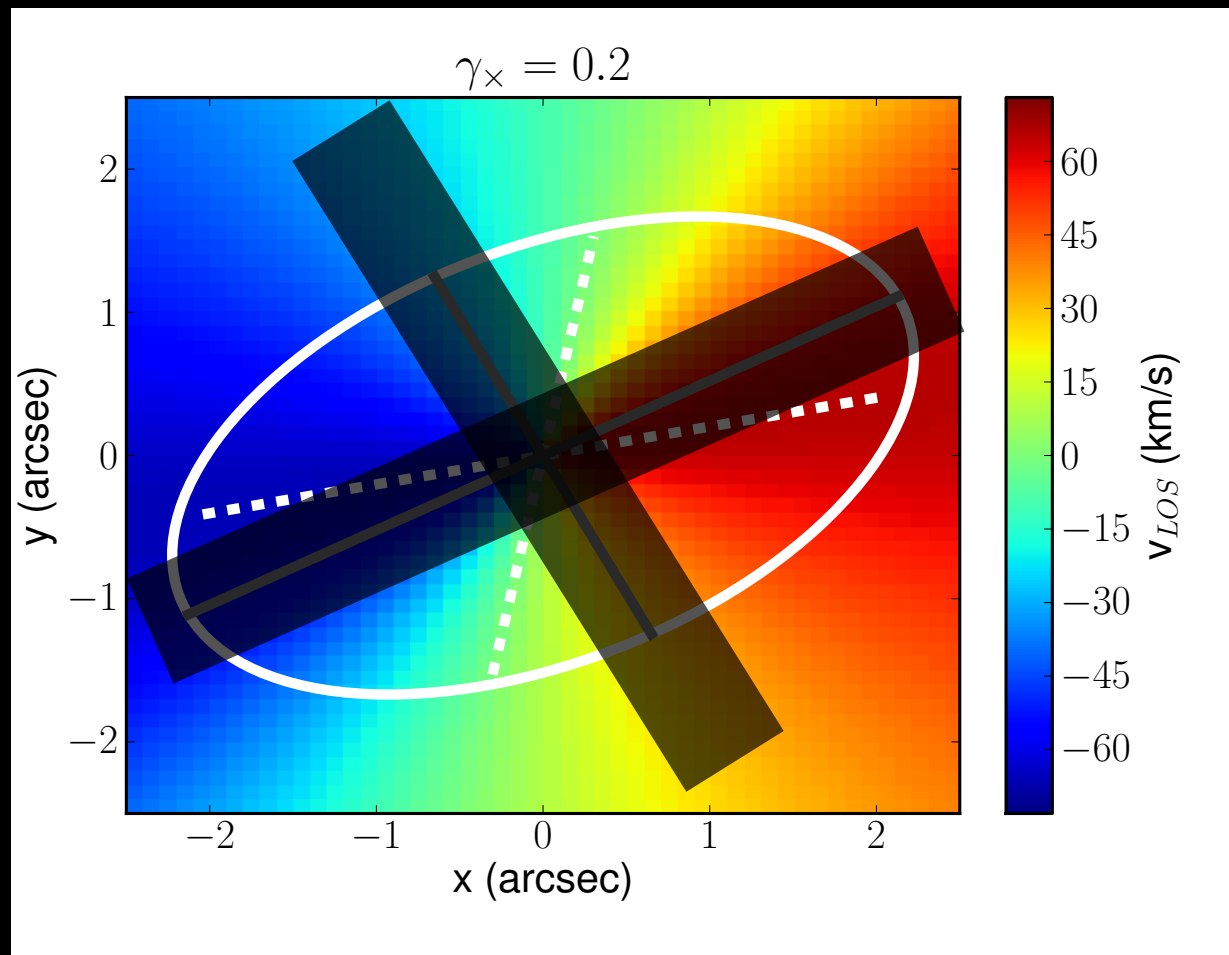
$$n_{\text{gal}} \approx .25 \text{ gal arcmin}^{-2}$$

$$\sim 10^3 \text{ deg}^2$$

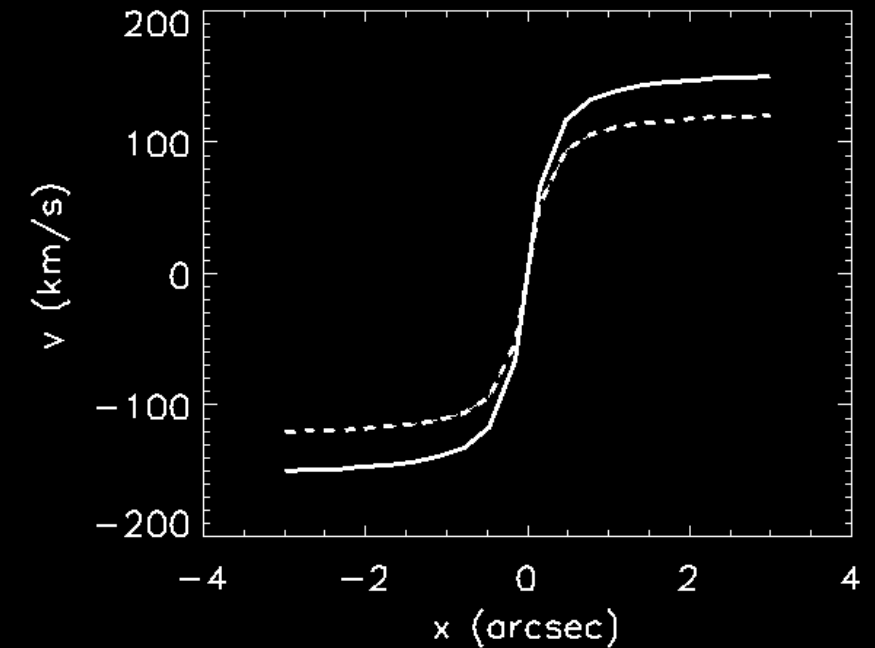
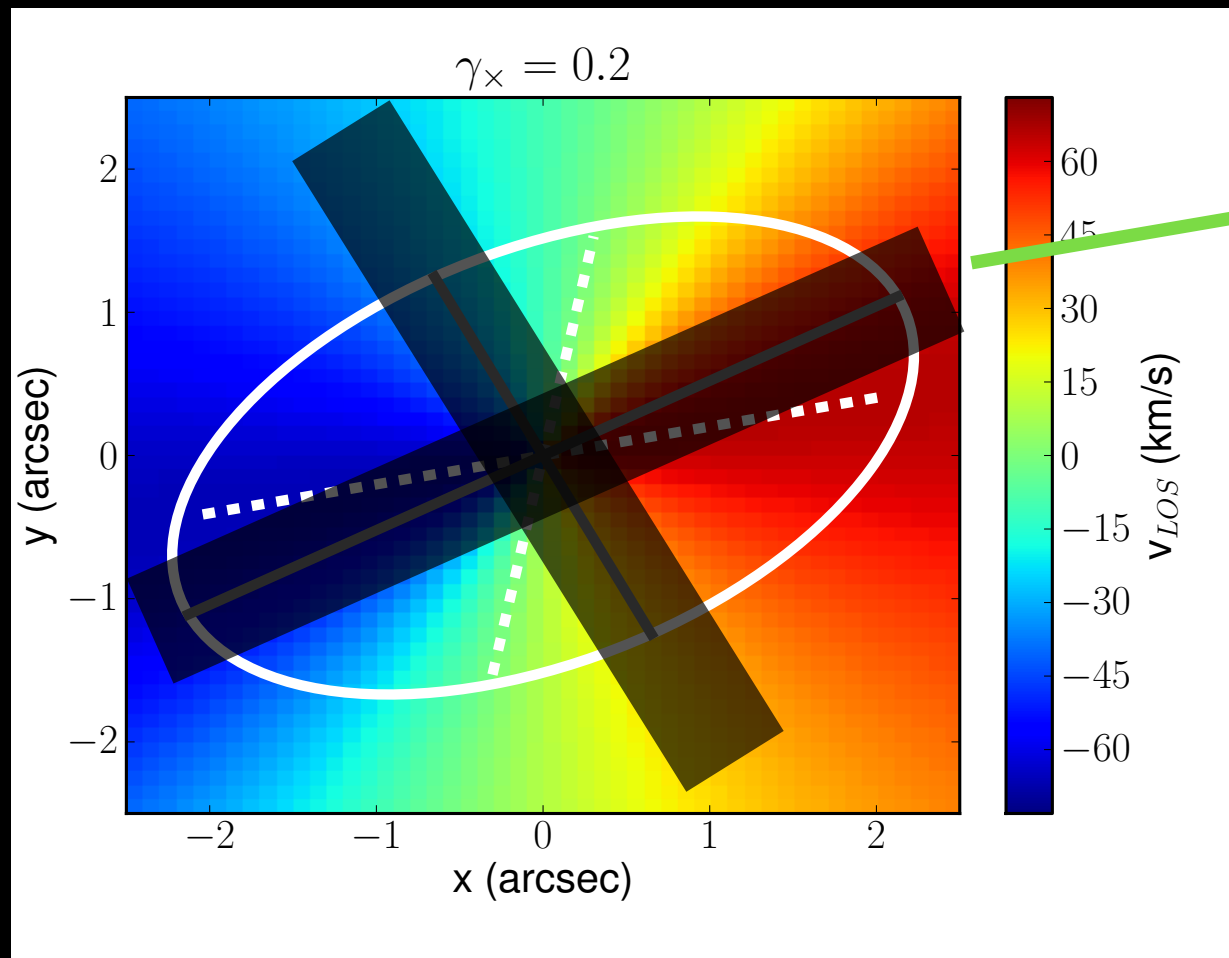
$$\implies 10^7 \text{ spectra}$$

This is comparable to PFS or DESI.

# A spectroscopic weak lensing measurement with slit spectroscopy



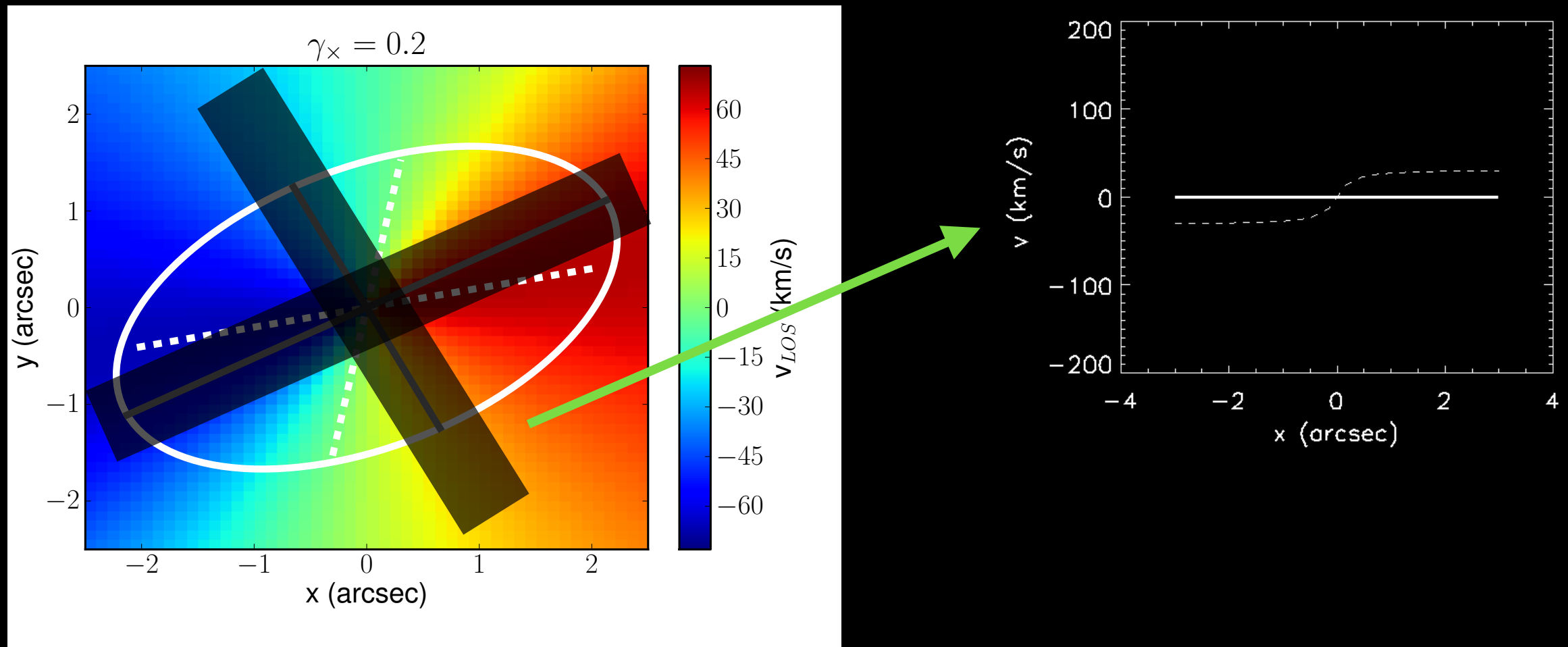
# A spectroscopic weak lensing measurement with slit spectroscopy



Less rotation along the major axis than TFR would predict

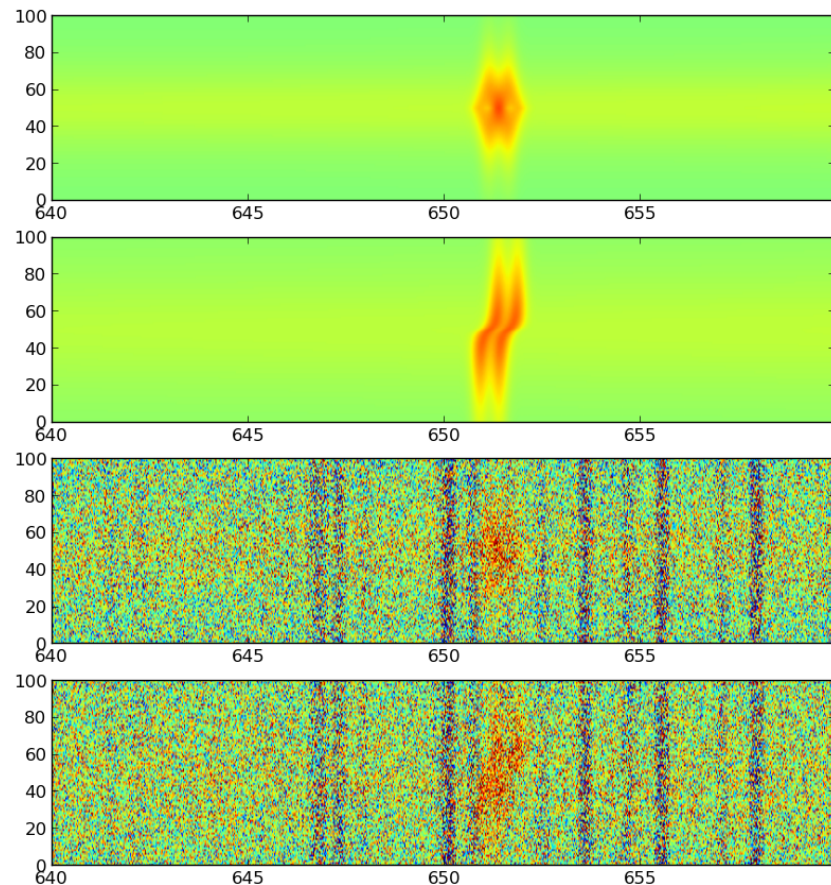


# A spectroscopic weak lensing measurement with slit spectroscopy



More rotation along the minor axis than TFR would predict

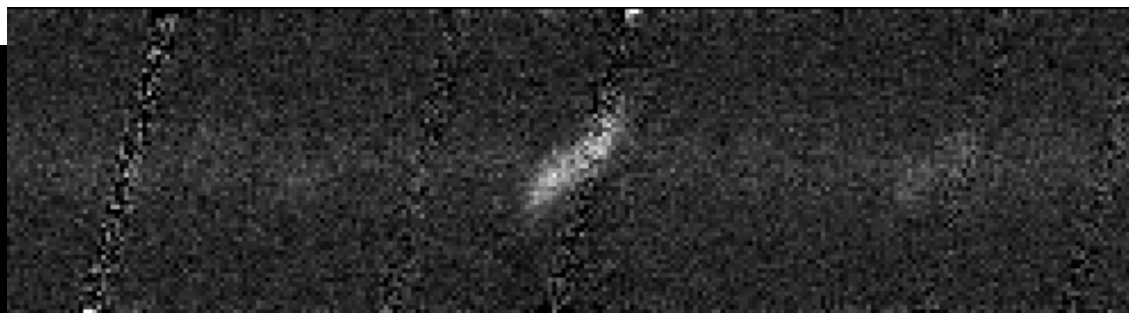
# Simulating the measurement: Slit Spectroscopy



simple galsim-based  
simulation

---

consistent with  
DES/DESI exposure  
time calculations

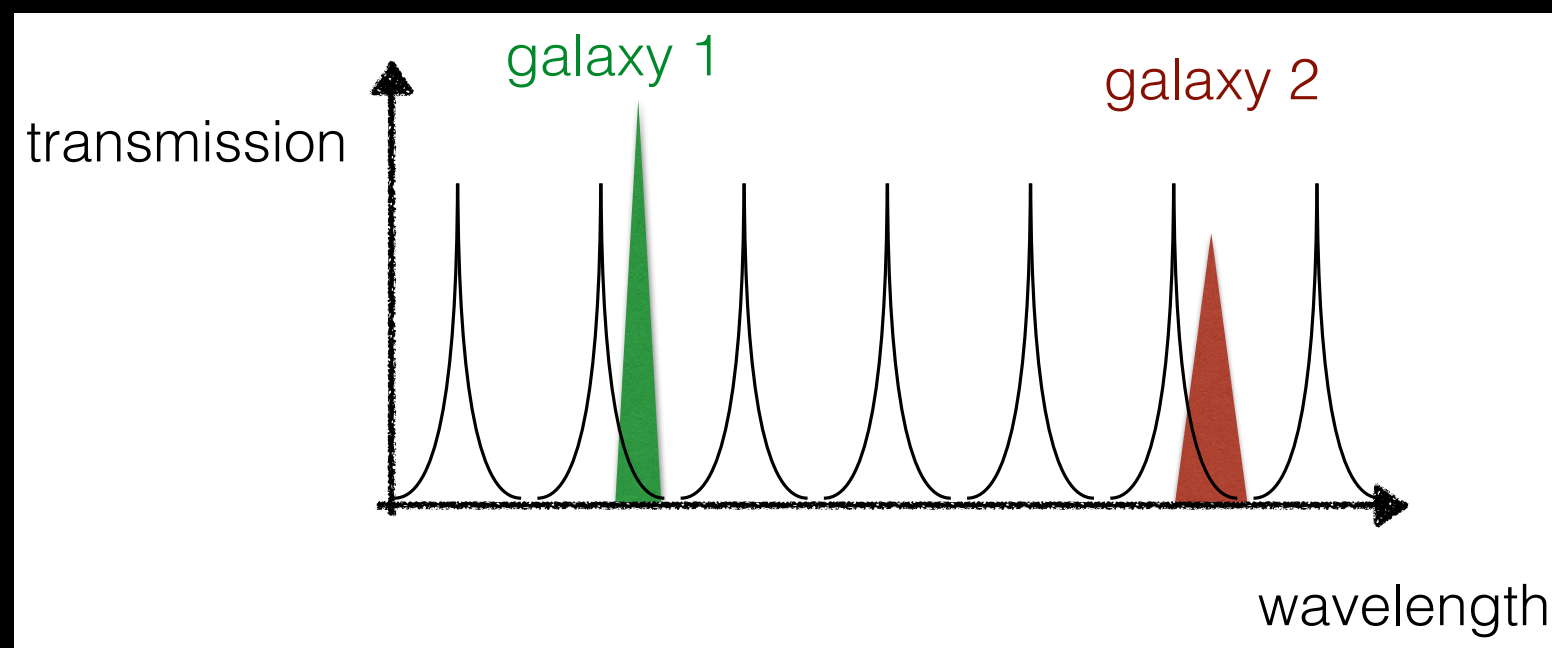
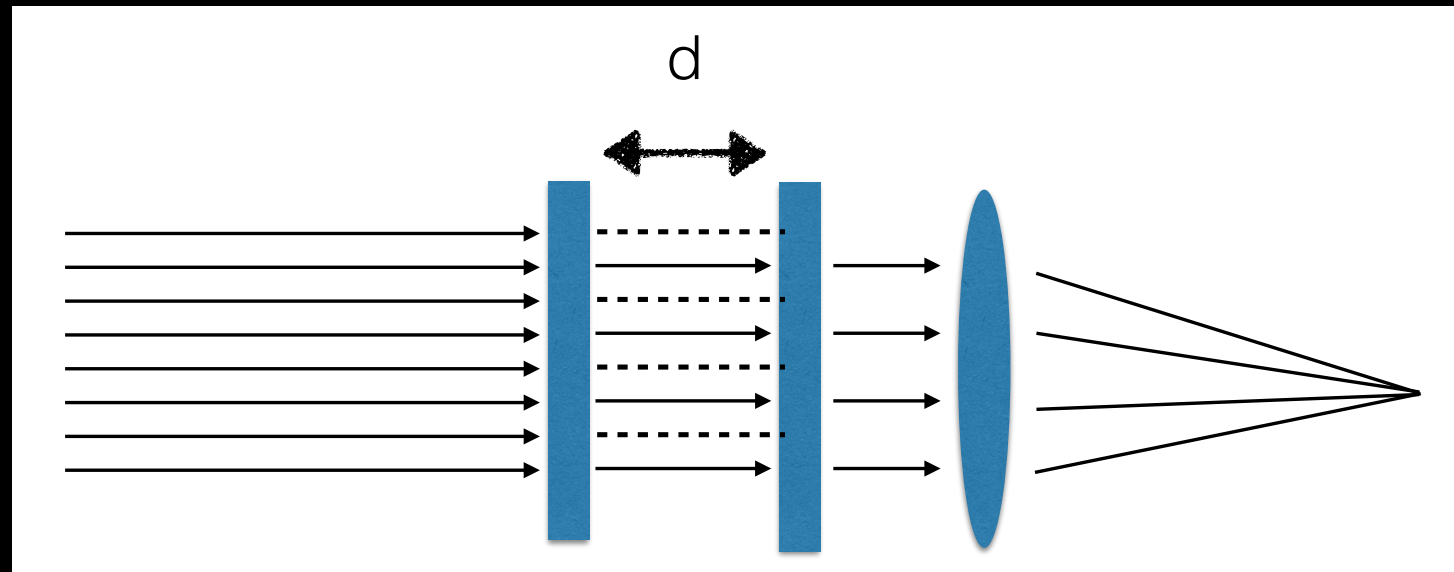


Keck-DEIMOS

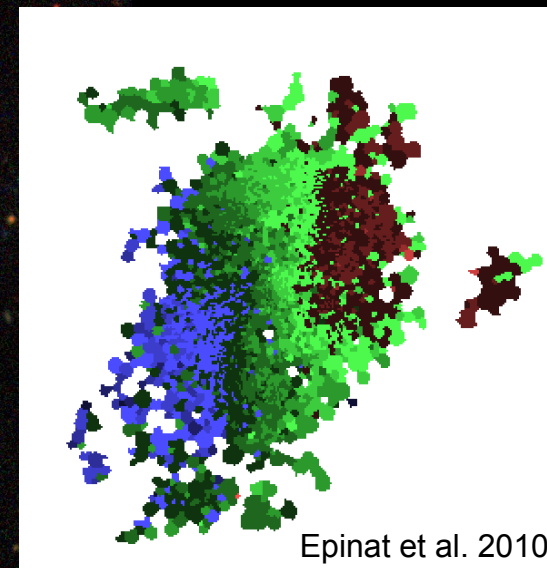
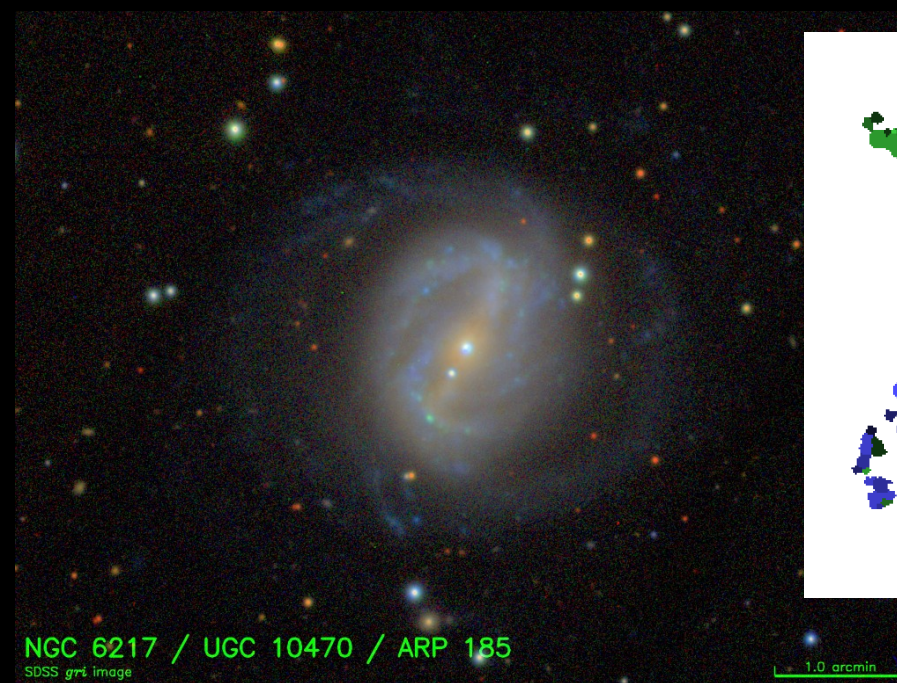
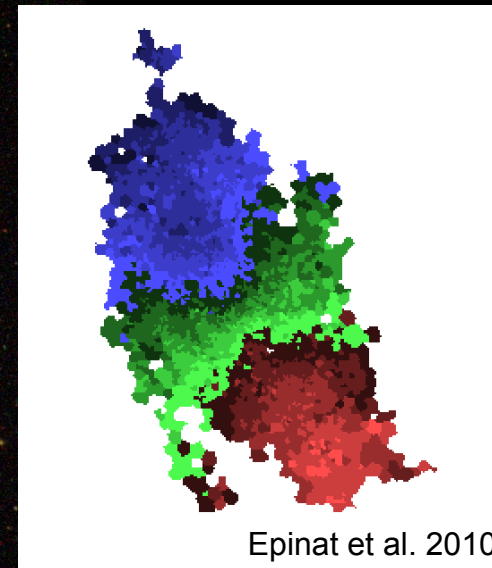
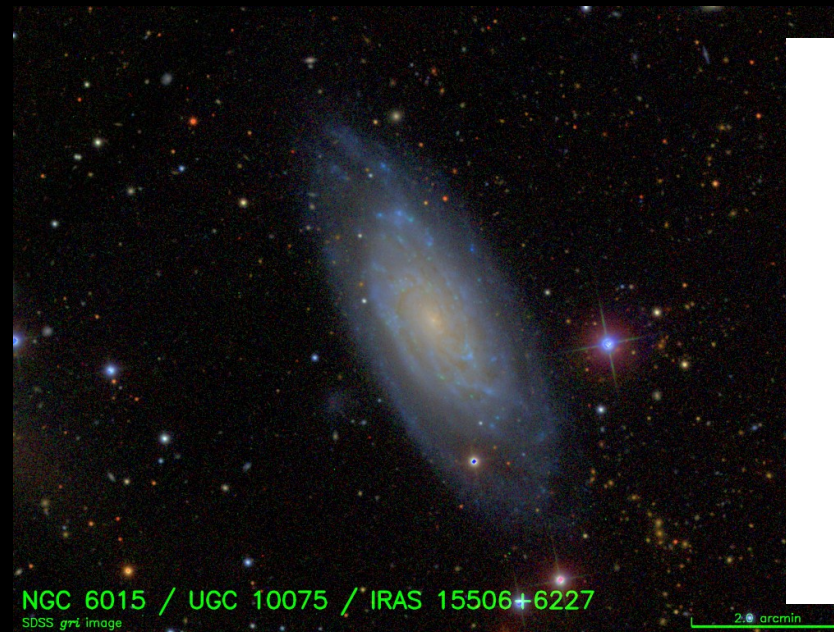
But *spatially resolved*  
slit spectroscopy does not scale to wide-field surveys.

We need hyperspectral imaging.

# One possible solution: Imaging Fabry-Perot Interferometer



# Example: GHASP survey data





# Massively Multiplexed Galaxy Kinematics from space

SPECTRE: A Fabry-Perot Imager concept

## Concept

- square-degree FP imager
- meter-class telescope with 0.1" resolution
- H-alpha kinematics to  $z < 0.5$
- ~all-sky survey

## Science

- Kinematic Lensing
- Peculiar Velocities
- Resolved kinematics of star forming regions

Survey	Number of galaxies (millions)	Spectral resolution elements per galaxy	Spatial resolution elements per galaxy	Total independent resolution elements (billions)
LSST	1,700	6	9	90
WFIRST (imaging)	320	3	400	380
WFIRST (grism)	20	600	1	12
SDSS	2	2,000	1	4
DESI	20	4,000	1	80
SPHEREx	450	130	1	60
Euclid (imaging)	1,620	1	100	160
<b>Total:</b>				<b>800</b>
<b>SPECTRE</b>	80	10,000	100	<b>80,000</b>

Table 1: Relative measure of information content of selected wide-field surveys, counting the number of usable galaxy targets and the spatial and spectral resolution of each.

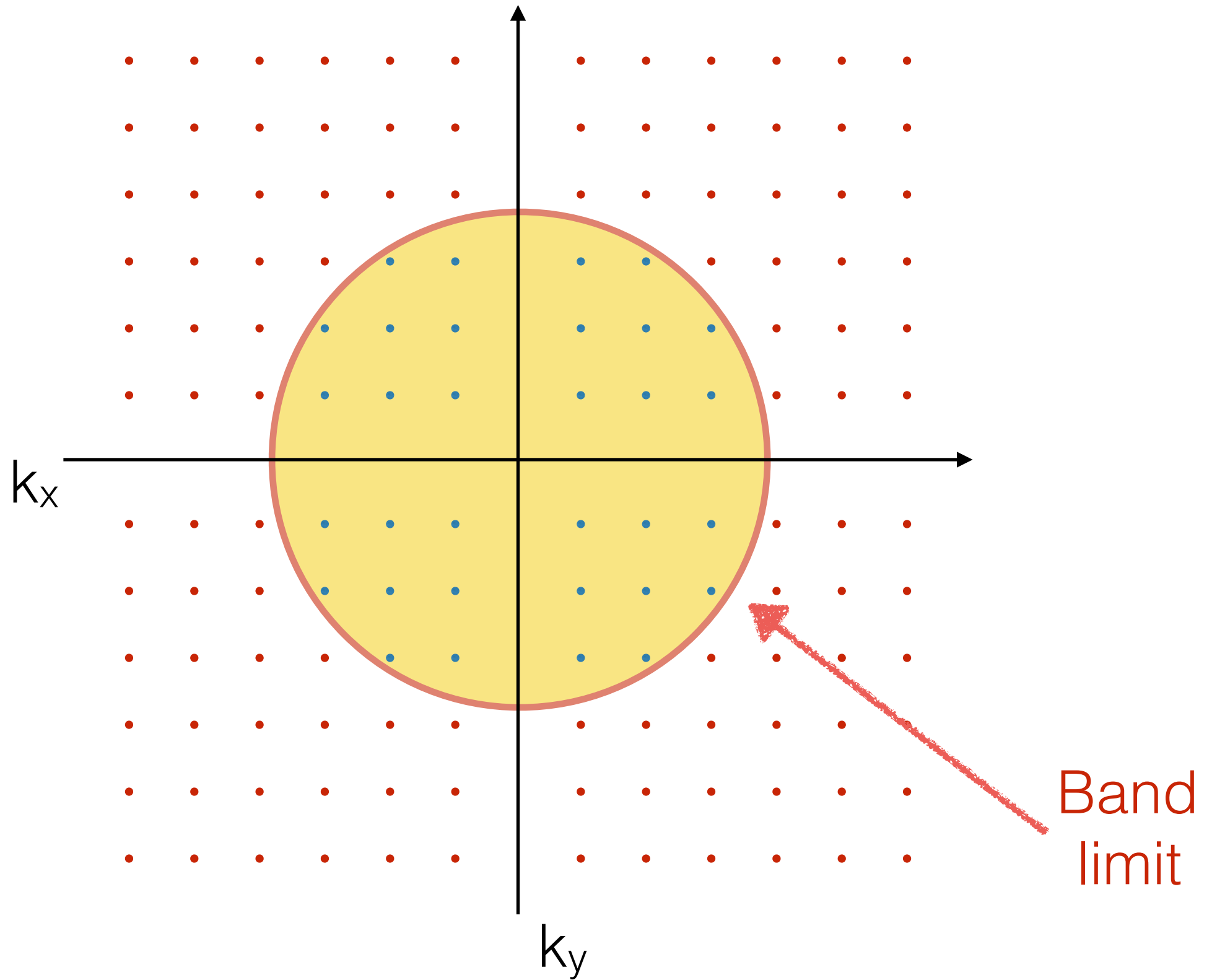


**Jet Propulsion Laboratory**  
California Institute of Technology

---

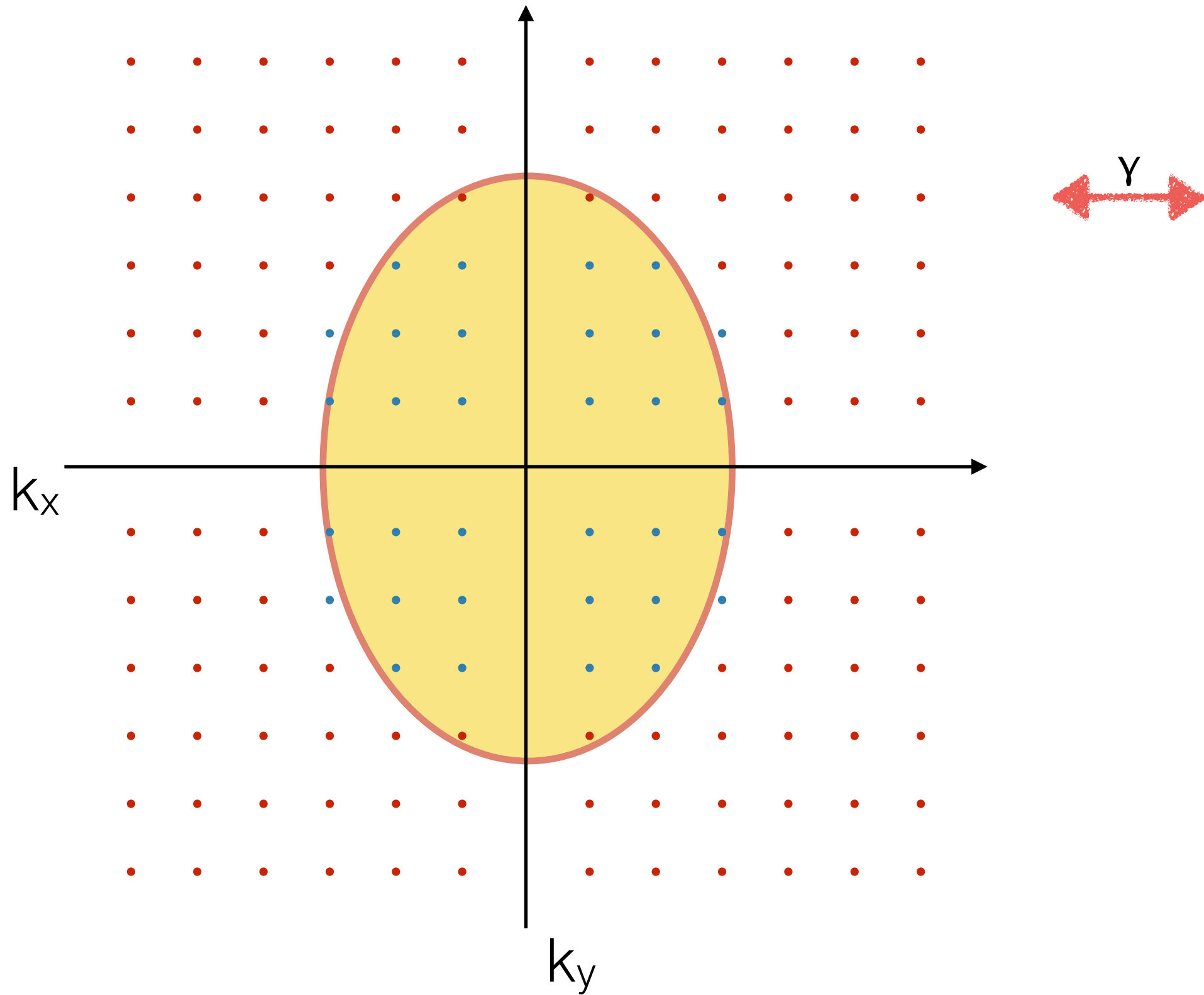
[jpl.nasa.gov](http://jpl.nasa.gov)

# Shear response depends on unresolved modes

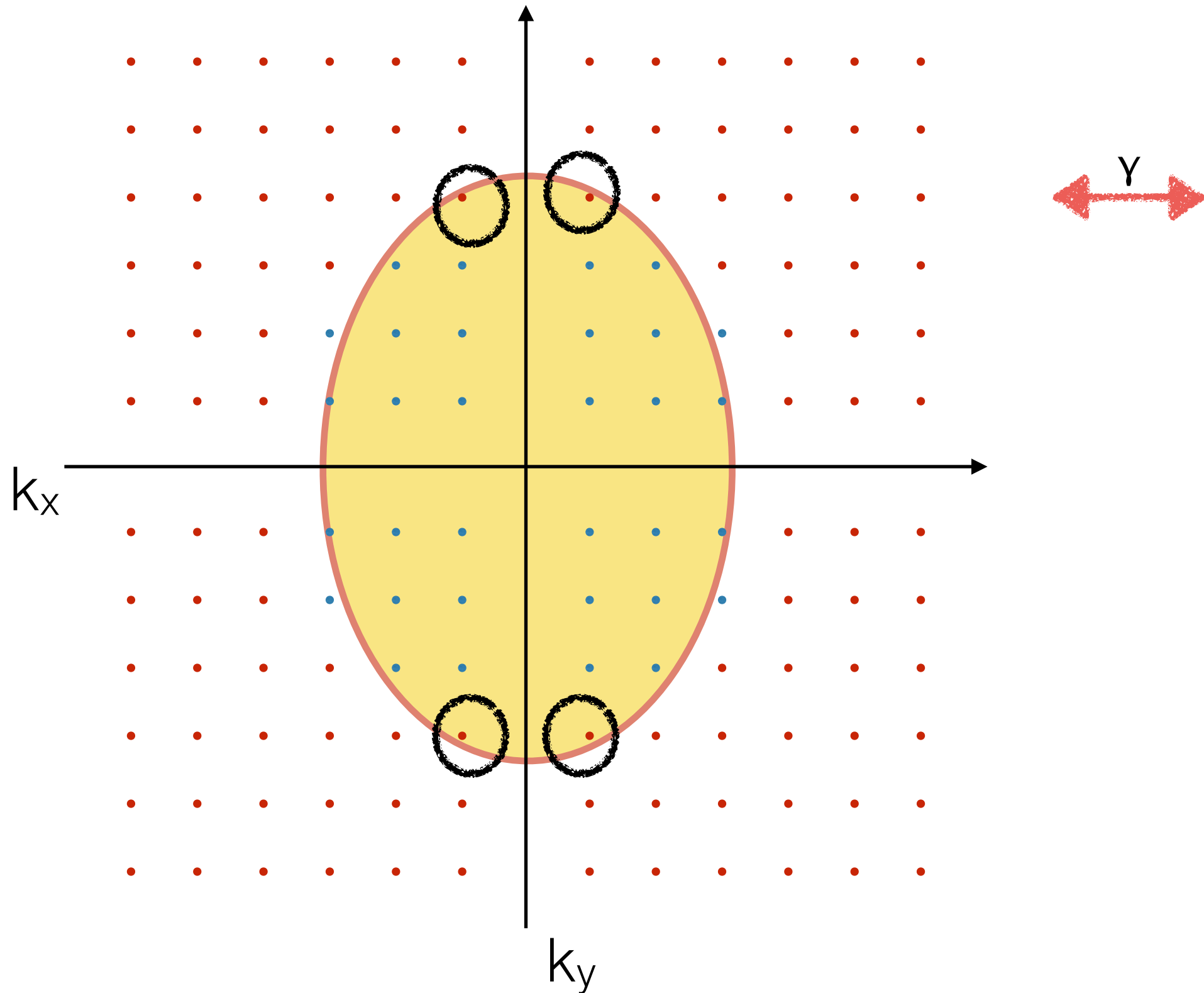




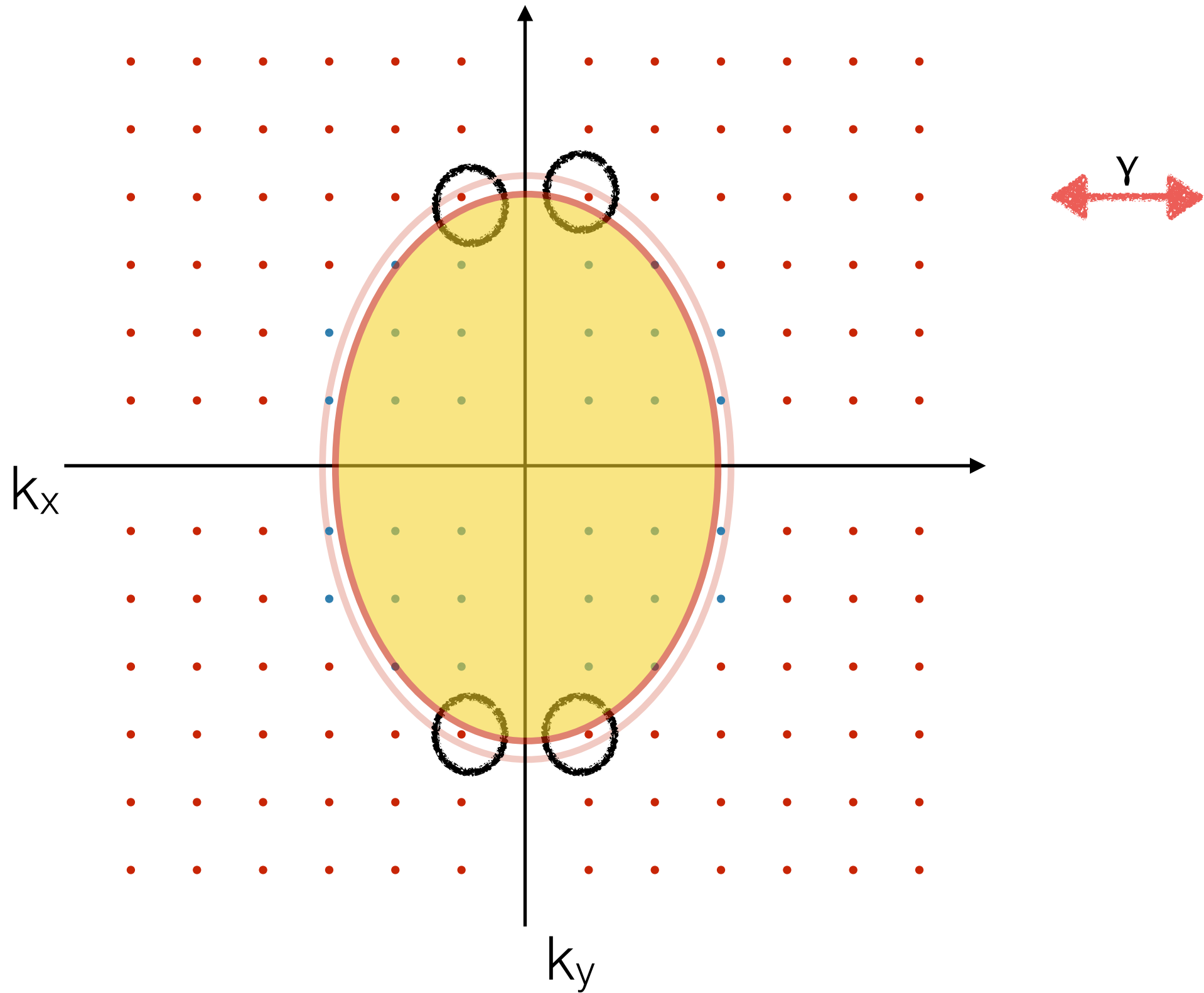
# Shear response depends on unresolved modes



# Shear response depends on unresolved modes

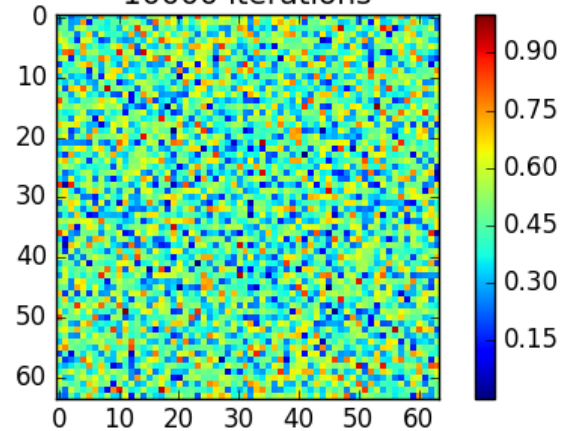


# Convolve to larger PSF to 'hide' noisy modes

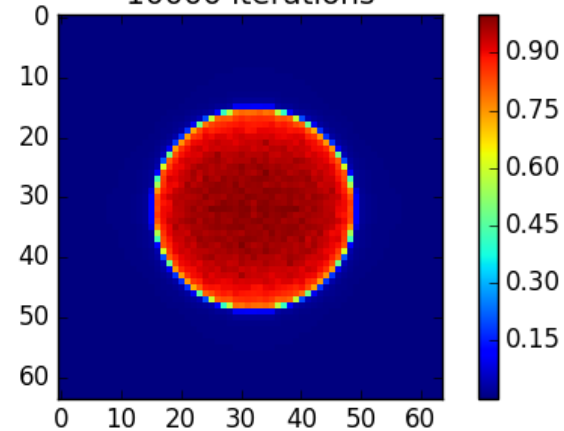


# Reconvolution+shearing modifies the noise field.

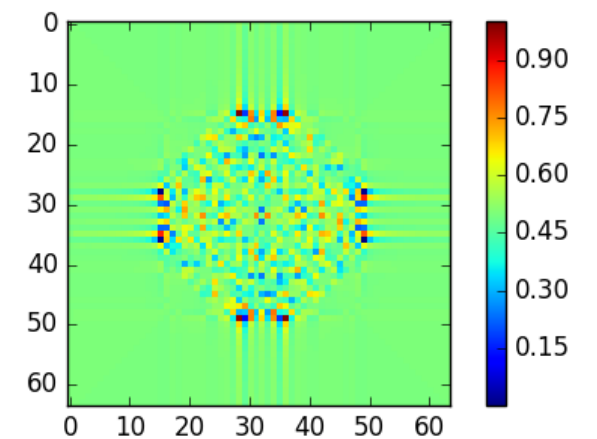
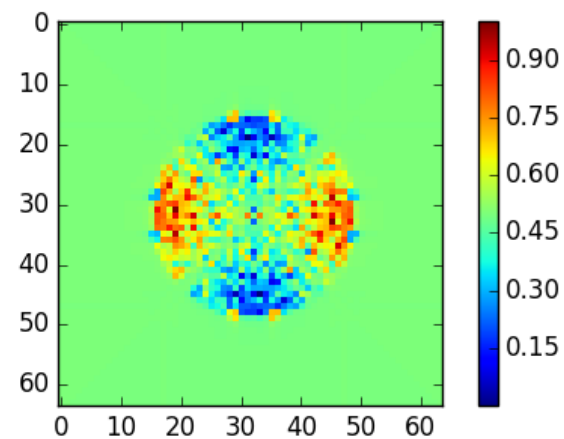
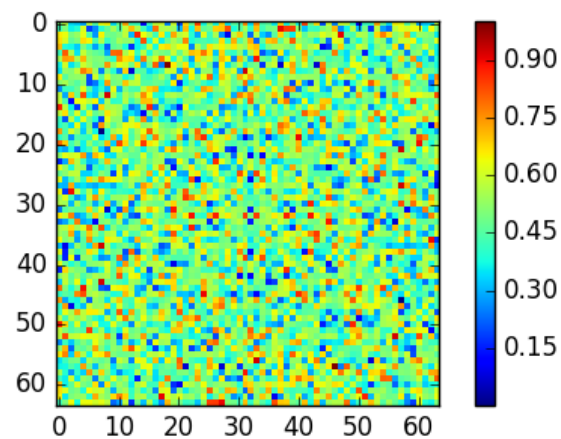
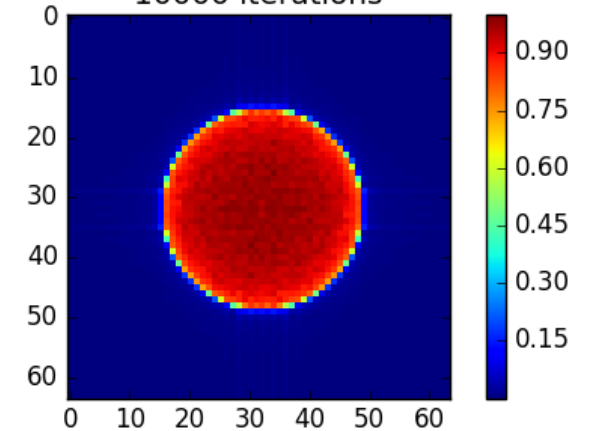
averaged white noise power,  
10000 iterations



averaged mcal noise power,  
10000 iterations



averaged mcal symm. noise power,  
10000 iterations



**We can mitigate by adding more noise, restoring symmetry.**

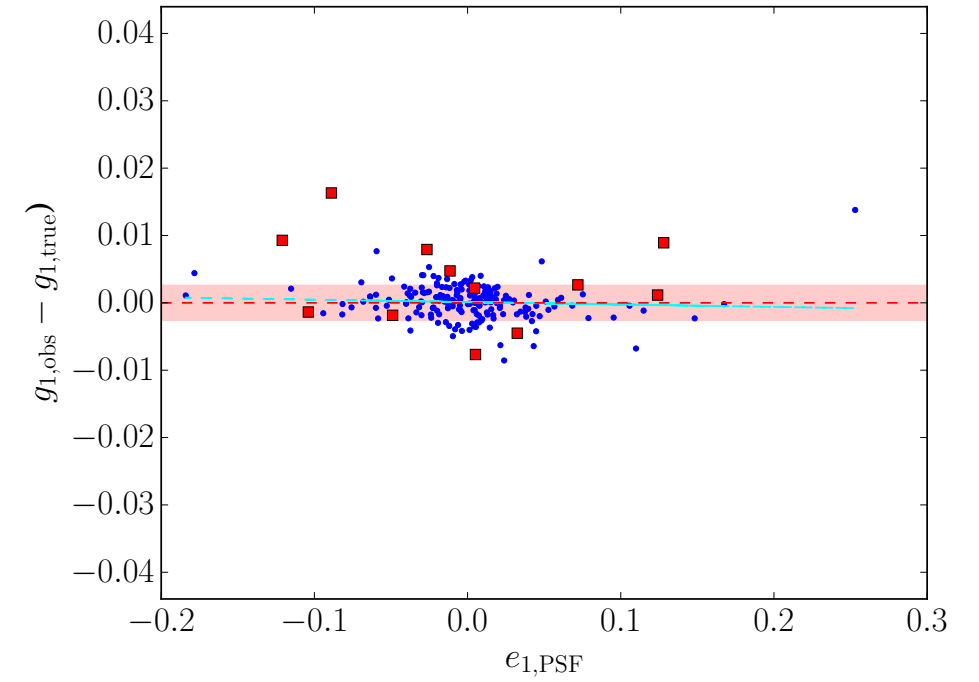
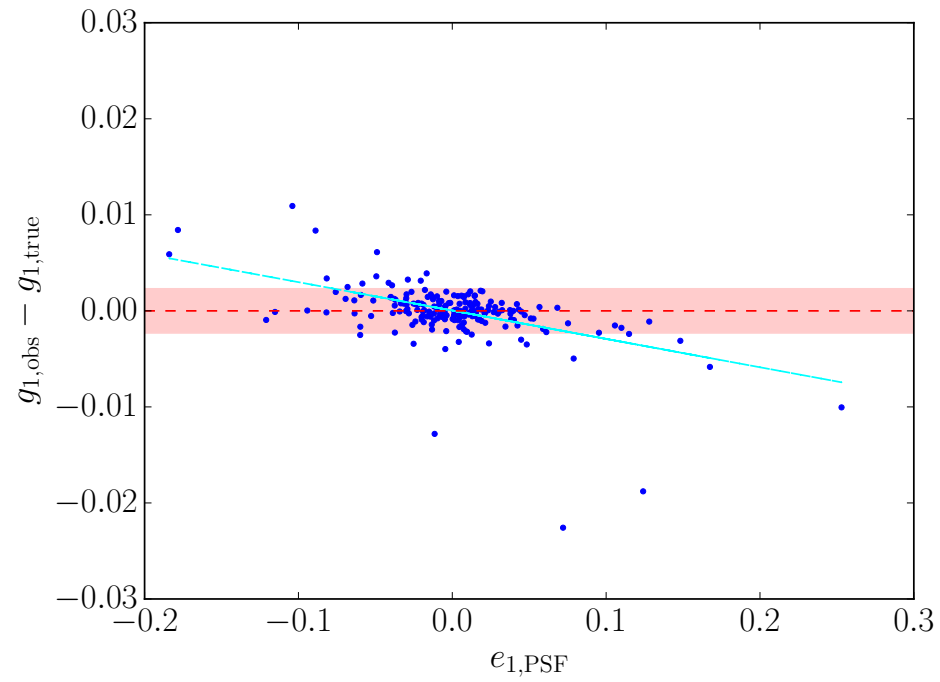
**Are there other useful ways to perturb the image?**

$$I'(x|e_{\text{PSF}}^+) = \Gamma^+ [P^{-1} * I]$$

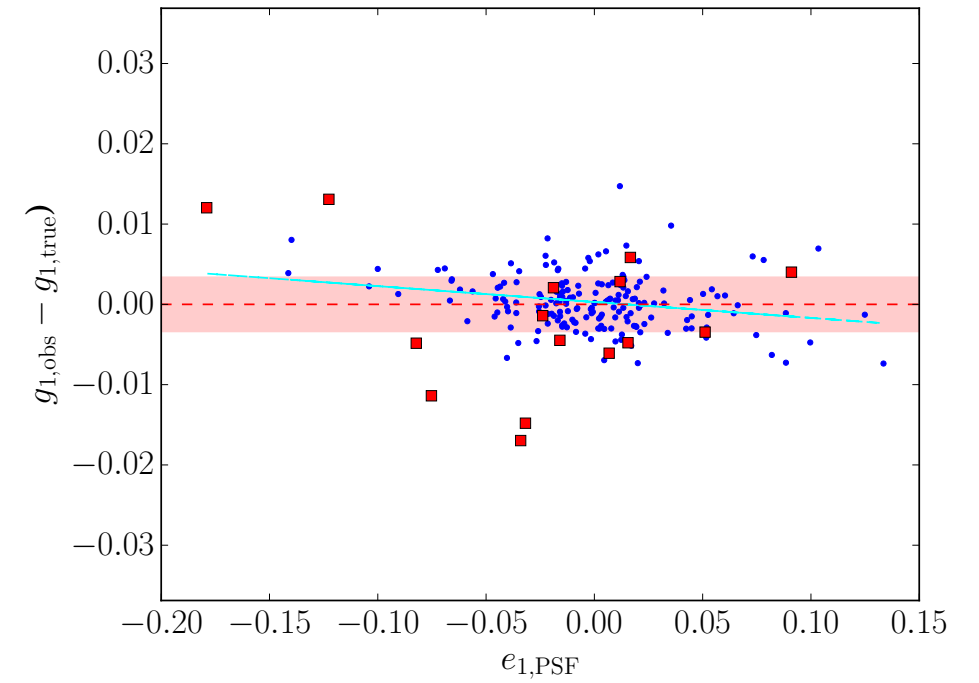
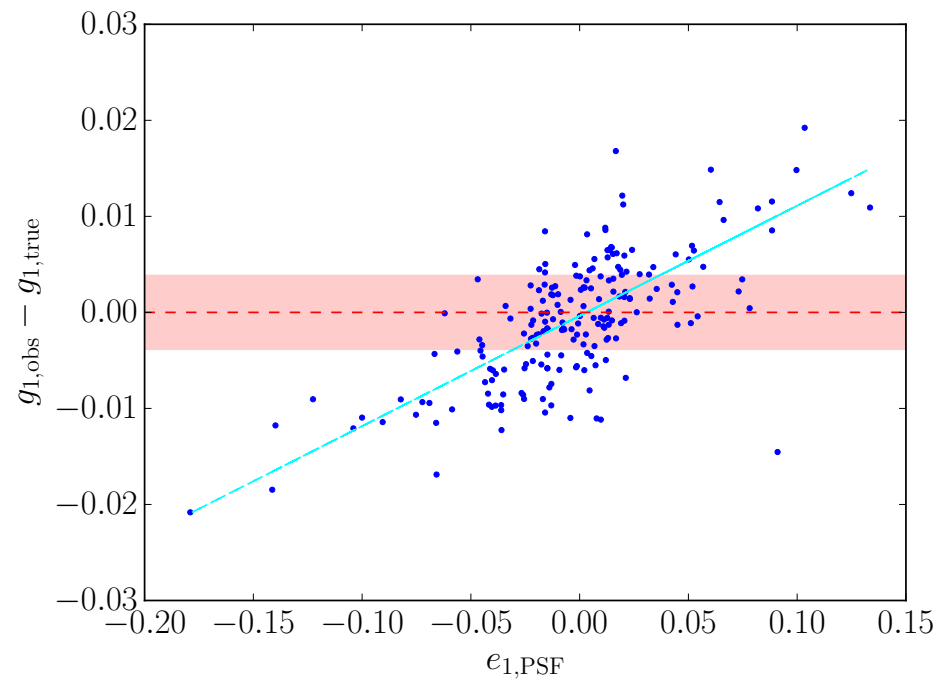
**We tried modifying the PSF. This could allow detrending of PSF correction errors.**

# PSF perturbation and detrending:

**KSB:**

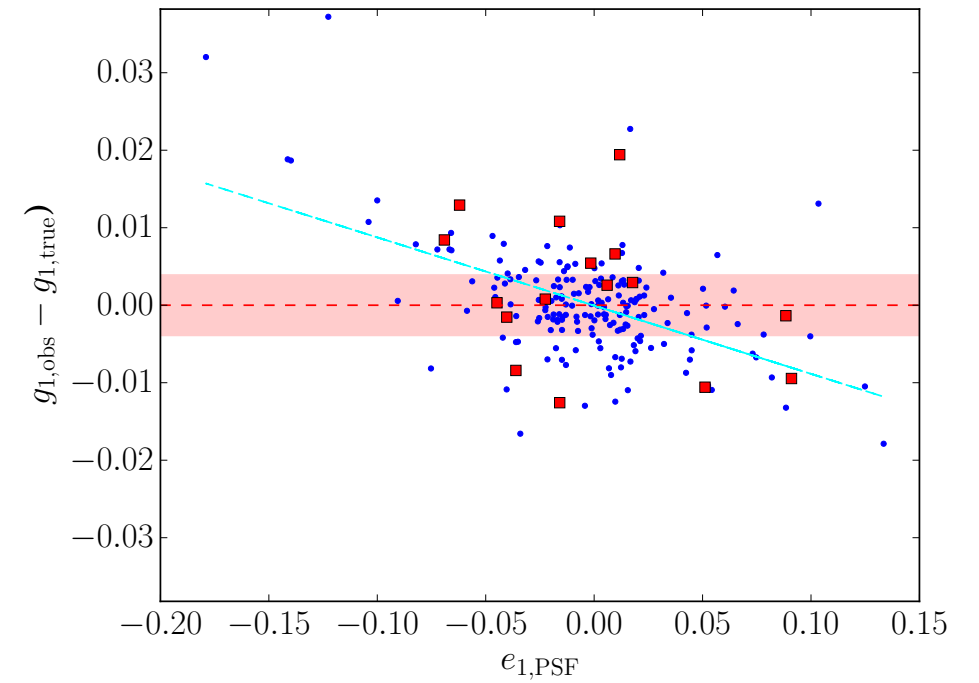
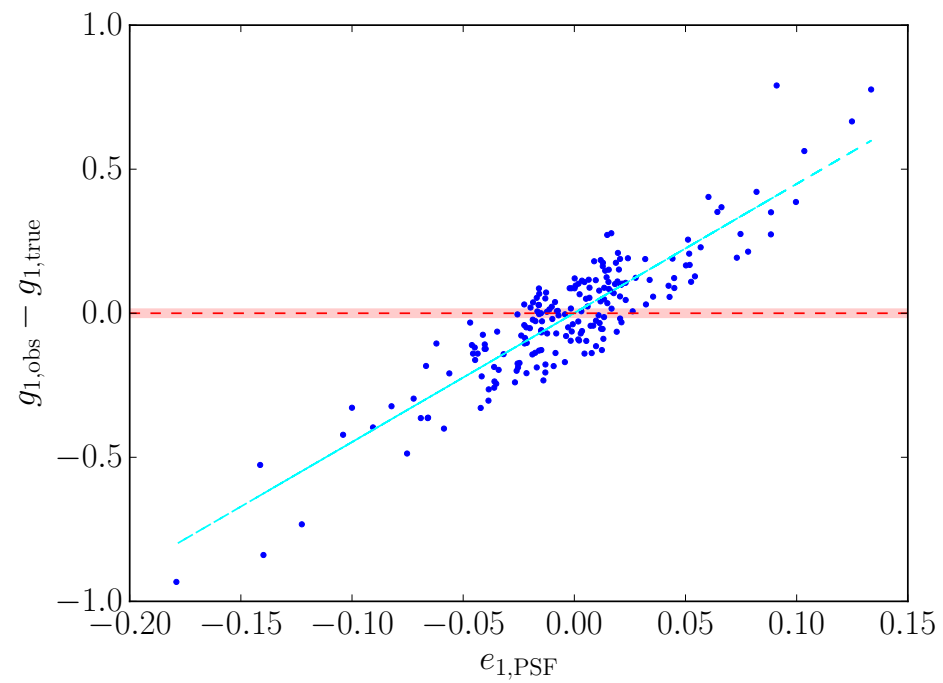


**regauss:**

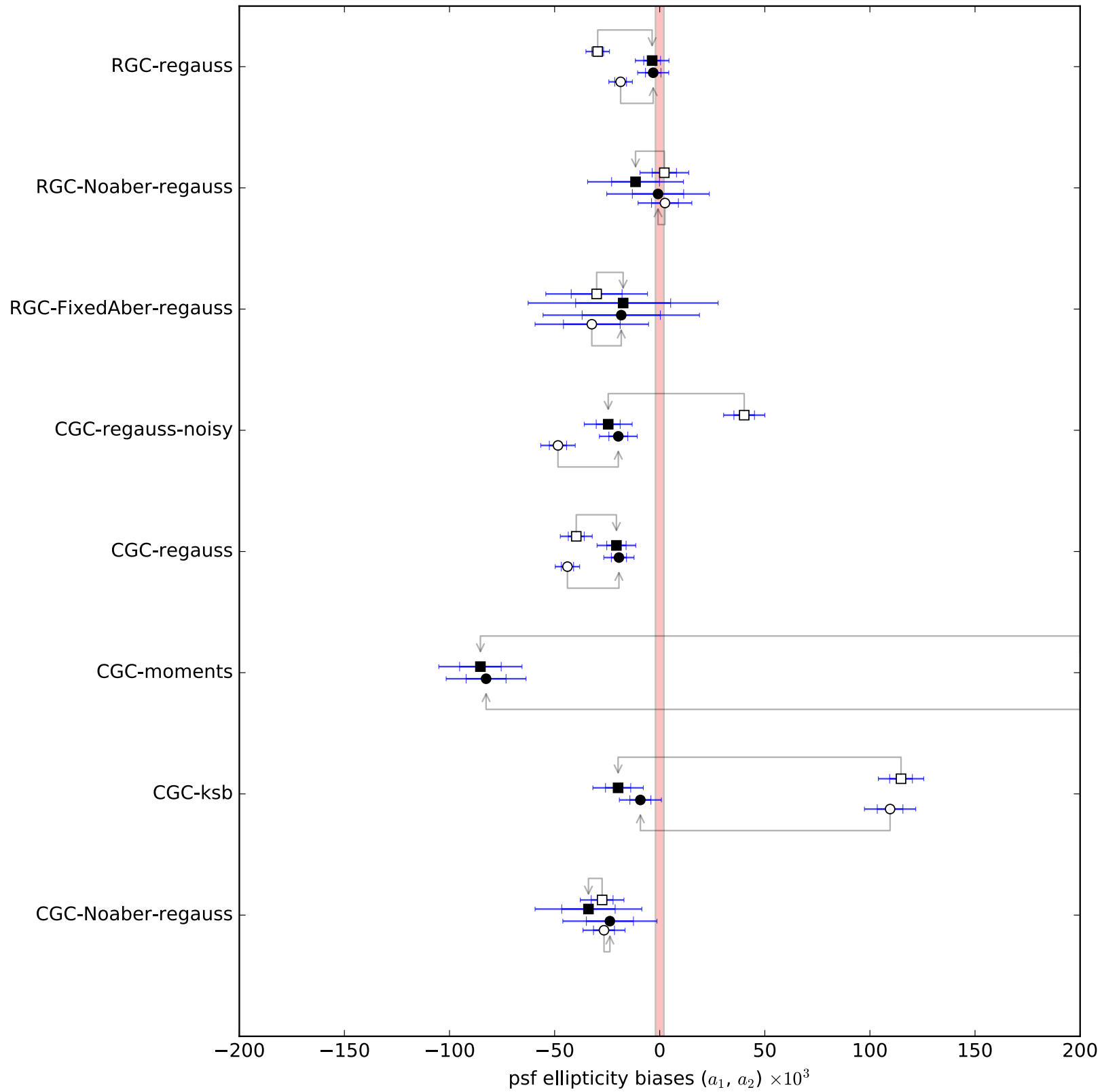


# PSF perturbation and detrending:

**moments:**



# PSF perturbation and detrending:





# **How to calibrate blends:**

# **How to calibrate blends:**

**1. Don't deblend.**

**(it's really a photo-z problem)**

# Correcting for selection effects:

$$\begin{aligned}\langle R \rangle &= \int \frac{\partial S(\mathbf{e}) P(\mathbf{e}) \mathbf{e}}{\partial \gamma} \Big|_{\gamma=0} d\mathbf{e} \\ &= \int \left[ S(\mathbf{e}) \frac{\partial P(\mathbf{e}) \mathbf{e}}{\partial \gamma} \Big|_{\gamma=0} + P(\mathbf{e}) \mathbf{e} \frac{\partial S(\mathbf{e})}{\partial \gamma} \Big|_{\gamma=0} \right] d\mathbf{e} \\ &= \frac{\langle e_i^+ \rangle^S - \langle e_i^- \rangle^S}{\Delta \gamma_j} + \frac{\langle e_i \rangle^{S+} - \langle e_i \rangle^{S-}}{\Delta \gamma_j}\end{aligned}$$

Apply a shear.

See how your measured shapes change.

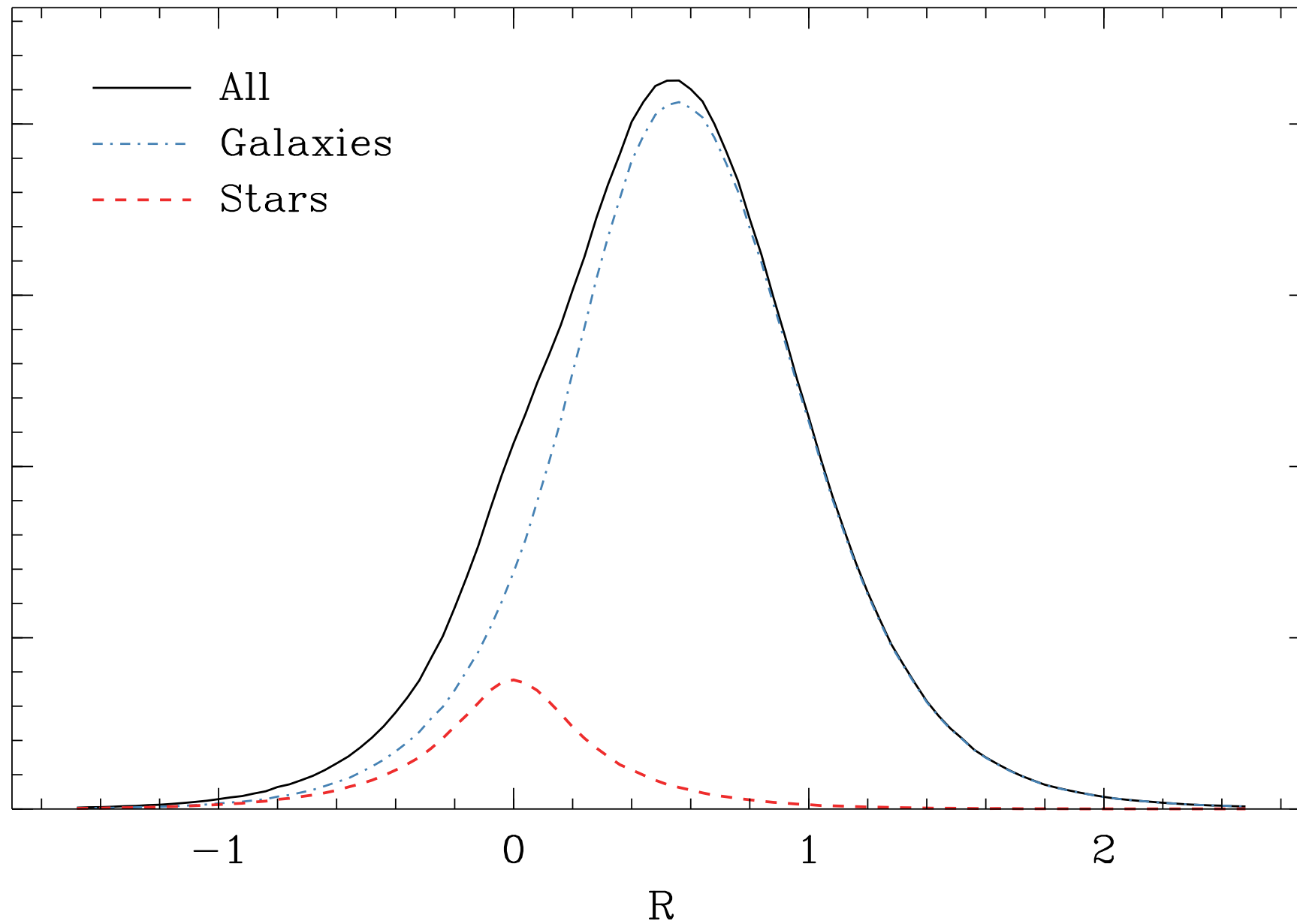
# Correcting for selection effects:

$$\begin{aligned}\langle R \rangle &= \int \frac{\partial S(\mathbf{e}) P(\mathbf{e}) \mathbf{e}}{\partial \gamma} \Big|_{\gamma=0} d\mathbf{e} \\ &= \int \left[ S(\mathbf{e}) \frac{\partial P(\mathbf{e}) \mathbf{e}}{\partial \gamma} \Big|_{\gamma=0} + P(\mathbf{e}) \mathbf{e} \frac{\partial S(\mathbf{e})}{\partial \gamma} \Big|_{\gamma=0} \right] d\mathbf{e} \\ &= \frac{\langle e_i^+ \rangle^S - \langle e_i^- \rangle^S}{\Delta \gamma_j} + \frac{\langle e_i \rangle^{S+} - \langle e_i \rangle^{S-}}{\Delta \gamma_j}\end{aligned}$$

Apply a shear.

See which galaxies enter and leave your sample.

# Imperfect star-galaxy separation does not appear to bias the inference.



# Peculiar Velocity Cross-Correlations

